ON THE RELATION BETWEEN LOCAL AND GLOBAL DAMAGE INDICES

by

E. DiPasquale[1] and A.S. Cakmak[2]

August 15, 1989

Technical Report NCEER-89-0034

NCEER Contract Number 88-1007

NSF Master Contract Number 86-07591

1 Research Associate, Dept. of Civil Engineering and Operations Research, Princeton University
2 Professor, Dept. of Civil Engineering and Operations Research, Princeton University

NATIONAL CENTER FOR EARTHQUAKE ENGINEERING RESEARCH
State University of New York at Buffalo
Red Jacket Quadrangle, Buffalo, NY 14261

PREFACE

The National Center for Earthquake Engineering Research (NCEER) is devoted to the expansion and dissemination of knowledge about earthquakes, the improvement of earthquake-resistant design, and the implementation of seismic hazard mitigation procedures to minimize loss of lives and property. The emphasis is on structures and lifelines that are found in zones of moderate to high seismicity throughout the United States.

NCEER's research is being carried out in an integrated and coordinated manner following a structured program. The current research program comprises four main areas:

- Existing and New Structures
- Secondary and Protective Systems
- Lifeline Systems
- Disaster Research and Planning

This technical report pertains to Program 1, Existing and New Structures, and more specifically to reliability analysis and risk assessment.

The long term goal of research in Existing and New Structures is to develop seismic hazard mitigation procedures through rational probabilistic risk assessment for damage or collapse of structures, mainly existing buildings, in regions of moderate to high seismicity. This work relies on improved definitions of seismicity and site response, experimental and analytical evaluations of systems response, and more accurate assessment of risk factors. This technology will be incorporated in expert systems tools and improved code formats for existing and new structures. Methods of retrofit will also be developed. When this work is completed, it should be possible to characterize and quantify societal impact of seismic risk in various geographical regions and large municipalities. Toward this goal, the program has been divided into five components, as shown in the figure below:

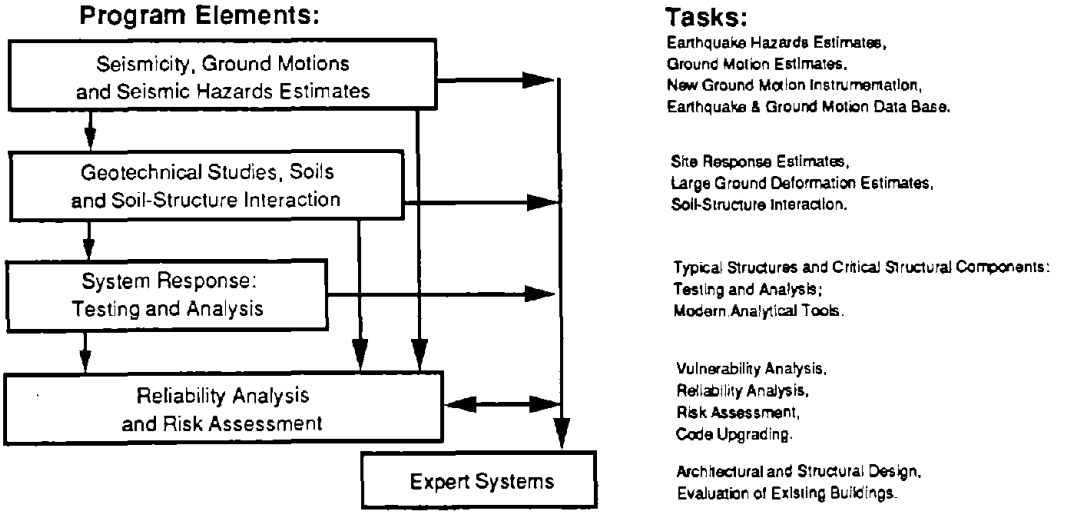

Reliability analysis and risk assessment research constitutes one of the important areas of Existing and New Structures. Current research addresses, among others, the following issues:

1. Code issues - Development of a probabilistic procedure to determine load and resistance factors. Load Resistance Factor Design (LRFD) includes the investigation of wind vs. seismic issues, and of estimating design seismic loads for areas of moderate to high seismicity.
2. Response modification factors - Evaluation of RMFs for buildings and bridges which combine the effect of shear and bending.
3. Seismic damage - Development of damage estimation procedures which include a global and local damage index, and damage control by design; and development of computer codes for identification of the degree of building damage and automated damage-based design procedures.
4. Seismic reliability analysis of building structures - Development of procedures to evaluate the seismic safety of buildings which includes limit states corresponding to serviceability and collapse.
5. Retrofit procedures and restoration strategies.
6. Risk assessment and societal impact.

Research projects concerned with reliability analysis and risk assessment are carried out to provide practical tools for engineers to assess seismic risk to structures for the ultimate purpose of mitigating societal impact.

This study shows that parameter-based global damage indices can be related to local stiffness degradation through operations of averaging over the body volume. The relationship obtained is applied to the case of numerical simulations of damage events as well as to the case of actual structures tested on shaking tables. Some results are also presented, relating parameter-based global damage indices to averages in space and in time of the local plastic strain. The relationship between local and global damage variables is also considered from an empirical point of view. Based on the analysis of a database of structures, a relationship between the apparent softening (global variable) of the structure and the interstory ductility (local variable) has been established. A set of fragility curves, relative to structural limit states, have thus been defined.

Abstract

Global damage indices based on equivalent modal parameters are defined. A structure exhibits a nonlinear behavior when it experiences a damaging earthquake. Nonetheless a time variant equivalent linear structure can be defined. An algorithm for the estimation of the modal parameters of a linear structure has been developed and implemented. Global damage indices are then defined from the vibrational parameters of the equivalent linear structure considered.

In Continuum Mechanics-based damage models, effects of the growth and coalescence of microcracks are accounted for through the definition of an internal or local damage variable. Damage to engineering materials essentially results in a decrease of the free energy stored in the body, with consequent degradation of the material stiffness. Strength degradation is also observed when plastic deformation occurs.

It is shown that parameter-based global damage indices can be related to local stiffness degradation through operations of averaging over the body volume. The relationship obtained is applied to the case of numerical simulations of damage events as well as to the case of actual structures tested on shaking tables. Some results are also presented, relating parameter-based global damage indices to averages in space and in time of the local plastic strain.

The relationship between local and global damage variables is also considered from an empirical point of view. Based on the analysis of a database of structures, subjected to simulated earthquake loads on the shaking table of the University of Illinois at Urbana-Champaign, a relationship between the apparent softening (global variable) of the structure and the interstory ductility (local variable) has been established. A set of fragility curves, relative to structural limit states, have thus been defined, providing the probability of exceedance of a given limit state as a function of the maximum softening.

Acknowledgements

This research was supported by a grant from the National Center for Earthquake Engineering Research, SUNY, Buffalo, NY. This support is gratefully acknowledged.

The authors are grateful to Prof. Attila Askar of Bogazici University, Istanbul, Turkey, and to Prof. Jenn-Wen Ju of Princeton University for the comments and suggestions that they have provided at every stage of this work.

TABLE OF CONTENTS

TABLE OF CONTENTS

LIST OF ILLUSTRATIONS

LIST OF TABLES

SECTION 1: INTRODUCTION

1.1. Definition of a Global Damage State

Most research in the field of damage assessment has dealt with the analysis of simple structural elements. The application of these techniques to the post earthquake analysis of existing structures is limited by the scarcity of data available in the field regarding the history of stress and strain for simple elements. In order to obtain such detailed information, in fact, a great number of instruments must be installed on the structure. Furthermore, when a certain degree of redundancy is present in the structure, local features of damage may not be very important in determining which, if any, repair actions should be carried out. Some average or global measures of damage may, in this case, be as useful to engineers as detailed information. Therefore, for the purpose of post-earthquake reliability assessment, it is convenient to define a global damage state for a structure that has experienced an earthquake. An intuitive approach is to define global damage as a combination of the damage at each point of the structure. The definition of "point" depends on the structural model that is chosen for the analysis. If the structure is modeled as an assemblage of beams in two or three dimensions, there will be $(\infty)^1$ points for which a damage state must be defined. If a complete 3-dimensional model is used, there will be $(\infty)^3$ points to be considered. The damage state can also be defined in several ways. One can think of a binary damage state (failure/no failure), or of a discrete valued damage state, using qualitative indicators such as safety, light damage, damage and critical damage (Stephens and Yao, 1987), or of continuous damage indices, as considered by Continuum Damage Mechanics. The damage state may or may not be dependent on the history of loads, depending on the particular model that has been chosen to describe the structural behavior (Kachanov (1958); Krajcinovic and Fonseca (1981); Lemaitre (1984)).

In general, therefore, a damage event that the structure undergoes can be described as a function

$$f : \mathbf{R}^n \rightarrow \mathbf{R}^n$$

The function f, which customarily takes values in the interval (0,1), is defined on the volume Ω occupied by the structure. f describes the loss of resistance experienced in the neighborhood of a given point. The global damage state D can thus be defined as a functional of f.

$$D = \int_{\Omega} w(\mathbf{x}) f(\mathbf{x}) \, d\mathbf{x} \tag{1.1.1}$$

where $w(\mathbf{x})$ is an appropriate weighting function.

This formulation of the damage problem, based on an infinite dimensional damage state, is theoretically correct but very impractical. The damage state must be reduced to a finite number of dimensions in order to solve the problem of damage assessment for a real structure. The need for this reduction was first pointed out by Yao (1982). It will be assumed therefore that a finite number of quantitative indicators is sufficient to determine the damage state of the whole structure. Such indicators are usually referred to as " damage indices". Once the number of dimensions has been reduced, the damage state of the structure can be inferred from the history of a finite number of structural parameters. The analysis of these histories yields numerical values for the corresponding damage indices.

The space of the damage indices can be termed "damage space". The expression (1.1.1) for the structure's damage can thus be simplified. If $\delta_1, ..., \delta_m$ are the damage indices considered, the global damage D is given by a function f defined on the damage space:

$$D = f(\delta_1,...,\delta_m) \tag{1.1.2}$$

Similarly a limit state will be defined as a surface g in the damage space:

$$g(\delta_1, ..., \delta_m) = 0 \tag{1.1.3}$$

Examples of limit states are the serviceability, or elastic, limit state, and the collapse limit state.

The reduction to a finite number of dimensions can be obtained by lumping procedures. The structure is modeled as an assemblage of elements and joints, for each of which a damage index is computed from the history of loading during the

earthquake. The global damage index for the structure is then defined as a weighted average of the damage indices for the single elements (Stephens and Yao, 1987; Park, Ang and Wen, 1985). If n_{el} elements and joints are considered, for each of them a damage index δ_i and a weight β_i can be defined, so that the global damage would be measured as:

$$\delta = \frac{1}{\sum_{i=1}^{nel} \beta_i} \sum_{i=1}^{nel} \beta_i \delta_i \qquad (1.1.4)$$

Reduction by lumping procedures requires that generalized displacements and restoring forces are available for a large number of nodes. This is possible in simulation studies, in the analysis of shaking table experiments, or for full scale structures that are extensively instrumented. In the practical case of a structure, where only two accelerometer arrays are installed, reduction by lumping is not directly possible.

The reduction procedure and the damage indices that are proposed in this report are based on the vibrational frequencies of the structure in the linear phase, and of an equivalent linear structure in the nonlinear phase. The functional form of the damage indices is derived from the theoretical and experimental analysis of damage of simple structural elements and of complex structures. It is shown that the proposed reduction is equivalent to an averaging operation of the damage variable, where the strain energy stored in the structure, for the mode shape corresponding to the frequency considered, is used as a weighting function.

1.2. Damage Indices Based on Equivalent Modal Parameters

A linear structural system described in terms of the modal parameters has been proved to be identifiable by Beck (1979). The modal parameters are the damping factor, natural frequency and effective participation factor for each natural mode, as considered in an approximate description of the structural motion based on modal

decomposition. When the structural behavior is nonlinear, the system identification algorithm based on linear models will yield estimates of equivalent linear parameters. When the structure enters a nonlinear phase, the equivalent linear model will change, reflecting the nonlinearities that take place during the strong motion. In particular, the structure will present an *apparent softening* as the amplitude of the oscillation increases, and the equivalent natural frequencies will decrease. By fitting a time variant linear model to the records, a history of the equivalent linear parameters is obtained. The algorithm used to estimate the equivalent parameters of a structure during earthquake strong motion has been presented by the authors in a previous publication (DiPasquale and Çakmak, 1987). The goal is now to extract information concerning damage from the history of the modal parameters. It is clear from the start that only the natural frequencies will provide valuable information. Damping factors are in fact entities of uncertain physical meaning, and their estimation, when the structure is in the nonlinear phase, yields results of questionable reliability.

In this paper, only the first (fundamental) natural frequency is considered. All the computations are actually carried out on its inverse, the fundamental period of vibration, because the fundamental period is the quantity most commonly considered in the engineering practice.

The interval $(0,s)$ of duration of the earthquake is divided into n_{wind} non-overlapping windows of width s_i seconds. For each of these windows, an equivalent fundamental period $(T_0)_i$ is computed. The first window can be made small enough, so that it can be assumed that the structure is still vibrating in the linear regime and that $(T_0)_1$ is equal to the fundamental period of the linear oscillation of the building before the earthquake, $(T_0)_{initial}$. When the record is long enough, so that the vibrations due to the strong motion have abated by the end of the record, and the behavior of the structure can be considered linear, the estimate of (T_0) corresponding to the last window, $(T_0)_{nwind}$, can be assumed to be equal to the fundamental period of the linear oscillation after the earthquake $(T_0)_{final}$. When the final portion of the record still presents apparent nonlinearities, $(T_0)_{final}$ can sometimes be obtained from post-earthquake tests.

Three parameters can thus be typically observed in the evolution of the equivalent fundamental period during an earthquake (see Figure 1.1, relative to the response of the Millikan Library in Pasadena, California, during the San Fernando earthquake, 1971). These are: (i) an initial value $(T_0)_{initial}$, which is assumed to correspond to the linear behavior of the undamaged structure, (ii) a final value $(T_0)_{final}$, corresponding to the linear behavior of the damaged structure, and (iii) the maximum value of the estimate of the fundamental period $(T_0)_{max}$, where the effect of nonlinear behavior and of soil-structure interactions is superimposed onto stiffness degradation.

Several indices can be proposed as measures of global structural damage. They are functions of the fundamental periods $(T_0)_i$ estimated during an earthquake, as well as of the initial fundamental period $(T_0)_{initial}$ and the final one $(T_0)_{final}$. The functional form of the indices may depend upon phenomenological aspects of damage at the local level, upon analytical considerations, and upon the analysis of data recorded from damaged structures.

When a single element (in the limit a single particle) of the structure is considered, several phenomenological aspects of damage should be taken into account. For reinforced concrete structures, attention should be concentrated on stiffness degradation and on plastic deformation. Other important phenomena that are believed to be linked to damage are the degradation of the strength and of the energy dissipation capacity of the element considered.

It is possible, as shown below, to compute averages of the local stiffness degradation using the vibrational parameters of the body, in particular $(T_0)_{final}$. The global stiffness degradation of a structure can thus be evaluated. A decrease in stiffness of some elements will result in a decrease of the natural frequencies of the structure (Rayleigh, 1894; Dowell, 1979). In particular, the fundamental period will increase. By comparing the fundamental period $(T_0)_{initial}$ and $(T_0)_{final}$ before and after the earthquake, a measure of the structure's global stiffness degradation can be obtained. The index thus defined will be called final softening and indicated with δ_f:

$$\delta_f = 1 - \frac{(T_0)^2_{initial}}{(T_0)^2_{final}} \tag{1.2.1}$$

The relation between δ_f and local stiffness degradation will be the subject of Section

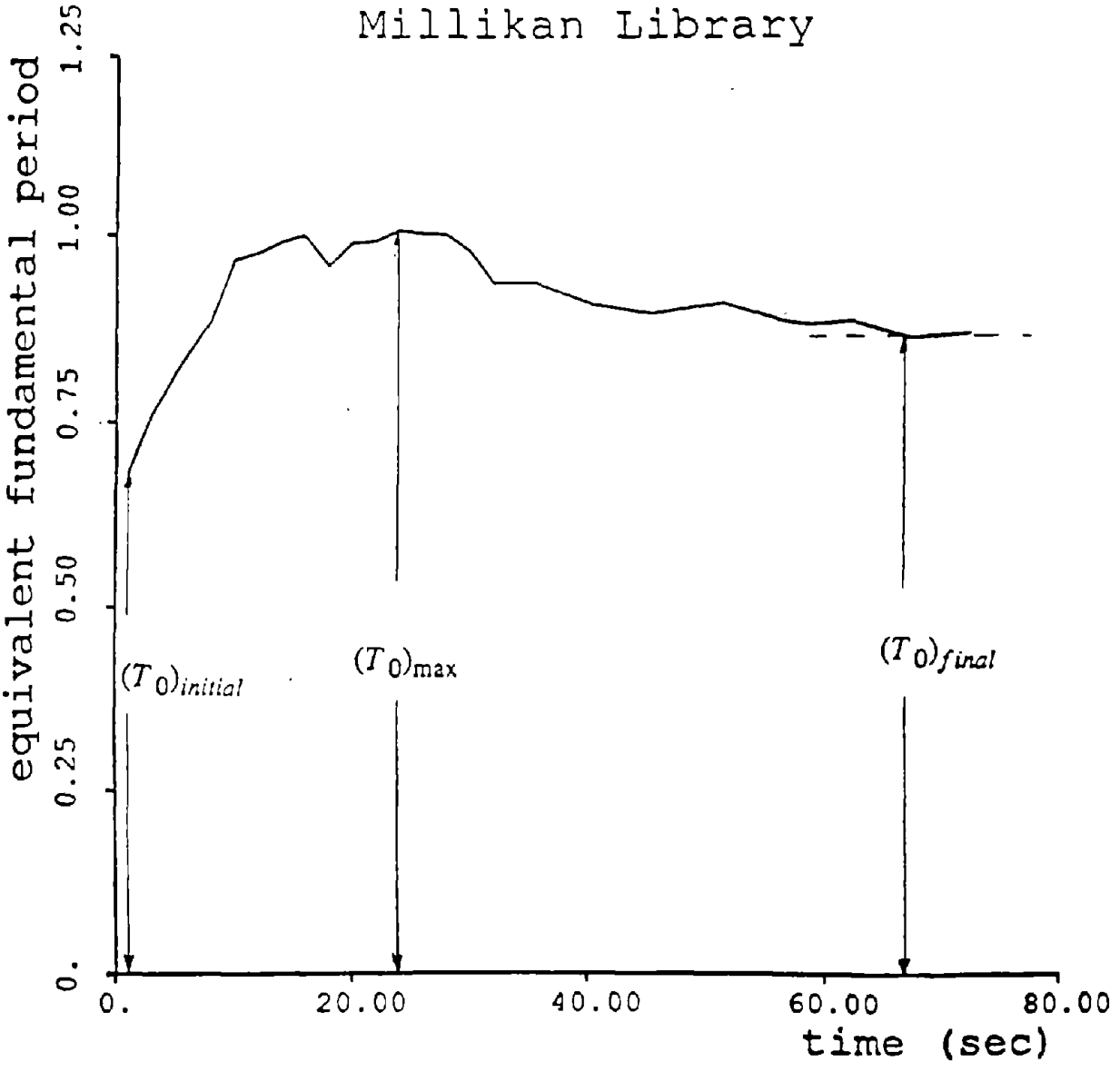

Figure 1.1: Evolution of the Equivalent Fundamental Period for the Millikan Library

3.

As has been pointed out before, during the strong motion, the effect of nonlinearities, such as plastic deformation, and of soil-structure interactions will appear as a softening of the equivalent linear structure, superimposed onto the softening due to stiffness degradation. In order to isolate these effects, the final (degraded) structure must be taken as a reference. A plastic softening is thus defined:

$$\delta_p = 1 - \frac{(T_0)^2_{final}}{(T_0)^2_{\max}} \tag{1.2.2}$$

The relationship between δ_p and the plastic deformation at the local level is analyzed in Section 4.

The contributions of stiffness degradation and permanent deformation to structural damage can therefore be identified. In order to clarify this statement, a typical restoring force characteristic for a reinforced concrete element can be considered. Figure 1.2 shows the shear-drift curve for a nonlinear story element. The restoring characteristic is trilinear. The first segment OA corresponds to the virtually undamaged material. When the element reaches the portion AB of the curve, tensile stress is experienced and cracks begin to appear. Beyond point B the steel reinforcements yield and plastic deformation takes place. If the element reaches any part of segment AB, the behavior in the subsequent loading/unloading cycles is still linear, but with a *degraded* stiffness (line OC). In a complex structure, if steel yielding does not appear in any element, $(T_0)_{final}$ will be equal to $(T_0)_{\max}$. The plastic softening (1.2.2) will therefore vanish and the final softening (1.2.1) will account for the global stiffness degradation. Permanent deformation is observed when the element reaches beyond point B on the restoring force curve. For the model considered, the unloading restoring characteristic, as well as the small vibration characteristic, will be parallel to the line OB (line DE in Figure 1.2). The comparison between $(T_0)_{final}$, determined by the small vibration characteristic, and $(T_0)_{\max}$, determined by the cycles of strain experienced by the structure, will provide a measure of the permanent deformation.

If the effect of stiffness degradation and plastic strain on the final damage state of the structure are assumed to be independent, a maximum softening δ_M can be defined as a

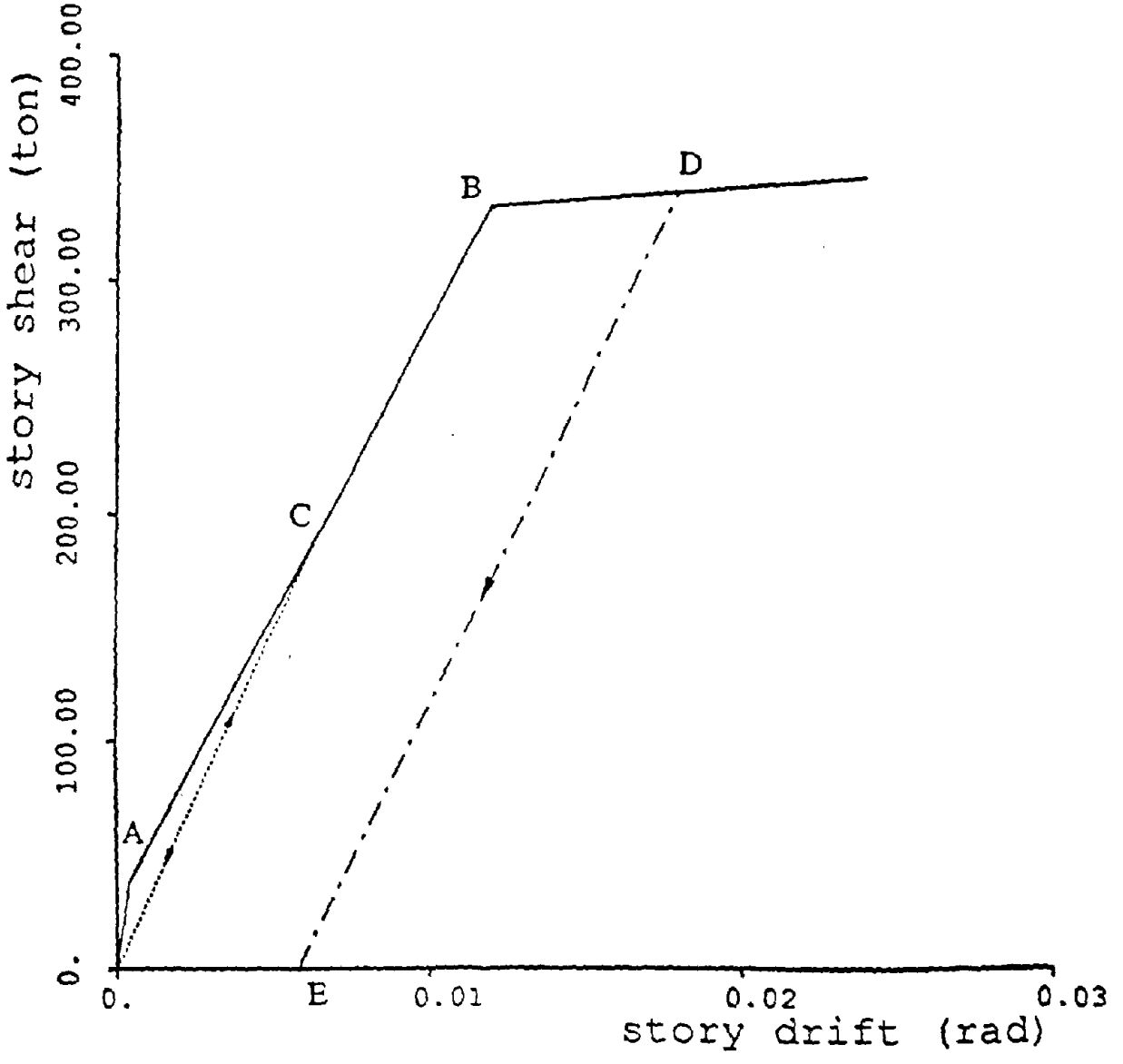

Figure 1.2: Restoring Force Characteristic for a Nonlinear Reinforced Concrete Elements

combination of δ_f and δ_p. The empirical analysis of seismic response of damaged structures, presented in Section 5, suggests a modification of the functional form of the damage indices, so that the contribution of the apparent softening to the structural damage appears now in a linear form:

$$\delta_M = 1 - \frac{(T_0)_{initial}}{(T_0)_{max}} \tag{1.2.3}$$

In section 5 it will be shown how δ_M can be related to the damage level of a structure.

1.3. Organization of the Work

Section 2 of this report briefly outlines the basic techniques of Continuum Damage Mechanics. In Section 3, the case of elastic damage is considered. A body experiences elastic damage when its restoring force characteristic degrades after a certain load history, with negligible permanent deformation. Some preliminary results, relative to the case of elasto-plastic damage, are presented in Section 4. Section 5 presents an engineering approach to damage assessment, linking customary local damage measures such as maximum interstory ductility with global parameter-based damage indices.

SECTION 2: ELEMENTS OF DAMAGE MECHANICS

2.1. Introduction

An introduction to Continuum Damage Mechanics (CDM) can be found in Lemaitre (1984), Krajcinovic (1984), and Kachanov (1986). The treatment presented here follows the approaches of Simo and Ju (1987a, 1987b) and of Ju (1988) (see also Ju et al., 1989). First, the basic hypotheses of Continuum Damage Mechanics are introduced. Then, a "total strain energy" based model for hyperelasticity coupled with damage is described. The case of plasticity coupled with damage is also considered.

From a microstructural standpoint, the progressive degradation of material properties results from the initiation, growth and coalescence of microcracks and microvoids. Within the framework of continuum mechanics, these processes may be modeled phenomenologically or micromechanically by introducing internal damage variables which correspond to these physical microprocesses. An internal damage variable can be a scalar or a tensorial quantity of the first, second or fourth order. Let us denote by $\mathbf{D}$ a fourth order anisotropic "damage" tensor which characterizes the state of damage of a generic unit cell. In general the mechanical behavior of anisotropic microcracks depends not only on their positions but also on their orientations. The transformation law from the homogenized or nominal stress tensor $\boldsymbol{\sigma}$ to the effective stress tensor $\bar{\boldsymbol{\sigma}}$ then takes the form:

$$\bar{\boldsymbol{\sigma}} = (\mathbf{I}-\mathbf{D})^{-1} : \boldsymbol{\sigma} \tag{2.1.1}$$

where $\mathbf{I}$ signifies the fourth order identity tensor. In essence, the effective stress concept implies that the effective stress $\bar{\boldsymbol{\sigma}}$ is the *true* stress experienced by the undamaged (virgin) material element. In other words, $\bar{\boldsymbol{\sigma}}$ is the stress which, if applied to the original undamaged material point, would give the same result as $\boldsymbol{\sigma}$ applied to the damaged material point. This statement will be formalized later in the "hypothesis of strain equivalence".

For the case of isotropic damage, the mechanical response of microcracks is independent of their orientations, depending only on a scalar variable d. Accordingly,

(**I**–**D**) reduces to $(1-d)$ **I** and (2.1.1) is rephrased as:

$$\bar{\sigma} = \frac{\sigma}{1-d} \tag{2.1.2}$$

where $d \in [0,1]$ is the damage parameter. It is noted that the value $d = 0$ corresponds to the undamaged state, a value $d \in (0,1)$ signifies a damaged state, and the value $d = 1$ corresponds to the complete failure of a local material element. Consequently, it is appropriate to interpret $[1-d]$ in Eq. (2.1.2) as a reduction factor associated with the amount of damage in the material. In fact, the damage variable d can be physically interpreted as the ratio of damaged surface area (corrected by stress concentration effects and interactions), A_d, over the total (nominal) surface area, A_T, at the point occupied by a material element; i.e.,

$$d = \frac{A_d}{A_T} \tag{2.1.3}$$

Equilibrium considerations then yield

$$(A_T - A_d)\,\bar{\sigma} = A_T\,\sigma \tag{2.1.4}$$

From (2.1.3) and (10), Eq. (2.2.1) is immediately obtained.

In addition to the effective stress concept, a "hypothesis of strain equivalence" is introduced by Lemaitre (1984):

> *"the strain associated with a damaged state under the applied stress is equivalent to the strain associated with the undamaged state under the effective stress".*

2.2. Elastic Damage Models

Materials such as cement paste, mortar and concrete are known to exhibit only small plastic deformations. As a consequence, the continuous degradation of material properties may be modeled in terms of the strain energy based "elastic-damage" models. For simplicity, the treatment here is restricted to isotropic damage (Eq. (2.2.1)). The damage models presented here are termed *"strain based"*. It is assumed that the damage in the material is directly linked to the history of total strain. Eqs. (2.1.1), (2.1.2) and the hypothesis of strain equivalence follow from this assumption, once an appropriate form for the free energy potential is defined.

A possible free energy potential accounting for isotropic damage coupled with hyperelasticity is:

$$\Psi(\boldsymbol{\varepsilon}, d) = (1-d)\,\Psi_0(\boldsymbol{\varepsilon}) \tag{2.2.1}$$

where $\boldsymbol{\varepsilon}$ denotes the infinitesimal strain tensor and $\Psi_0(\boldsymbol{\varepsilon})$ is the initial undamaged elastic strain energy function for a virgin material. For the special case of linear elasticity, for example, the undamaged free energy potential has the form:

$$\Psi_0(\boldsymbol{\varepsilon}) = \tfrac{1}{2}\,\boldsymbol{\varepsilon} : \mathbf{C}^0 : \boldsymbol{\varepsilon}$$

where $\mathbf{C}^0$ denotes the linear elasticity tensor. Assuming that only isothermal processes are considered, the reduced entropy production inequality requires then that

$$-\dot{\Psi} + \boldsymbol{\sigma} : \dot{\boldsymbol{\varepsilon}} \geq 0 \tag{2.2.2}$$

This leads to the following *damaged* stress-strain relation:

$$\boldsymbol{\sigma} = \frac{\partial \Psi}{\partial \boldsymbol{\varepsilon}} = (1-d)\,\frac{\partial \Psi_0}{\partial \boldsymbol{\varepsilon}} \tag{2.2.3}$$

along with the dissipative inequality

$$\Psi_0(\boldsymbol{\varepsilon})\,\dot{d} \geq 0 \tag{2.2.4}$$

In addition, it follows immediately from (2.2.1) (see also Lemaitre (1984)) that

$$-\frac{\partial \Psi}{\partial d} = \Psi_0(\boldsymbol{\varepsilon}) \tag{2.2.5}$$

The undamaged elastic strain energy function constitutes therefore the thermodynamic force conjugate to the damage variable. From Eq. (2.2.3) it can be easily seen that damage results in stiffness degradation at the local level. The elastic Young's modulus E and the shear modulus G of the damaged material element will be decreased by a factor $(1-d)$ with respect to the undamaged values E_0 and G_0. That is,

$$E = (1-d)\,E_0 \tag{2.2.6a}$$

$$G = (1-d)\,G_0 \tag{2.2.6b}$$

Progressive damage coupled with hyperelasticity can be characterized with a simple isotropic damage mechanism. In view of the above thermodynamical bases, the damage state can be defined through an "equivalent measure of strain energy", ξ, such as:

$$\xi \equiv [2\Psi_0(\epsilon)]^{\frac{1}{2}} \tag{2.2.7}$$

A strain space damage criterion then takes the form:

$$g(\xi, r) = \xi - r \leq 0 \tag{2.2.8}$$

where r denotes the current damage threshold. The initial damage threshold (before loading starts) is denoted by r_0, which is a property of the material. Analogous to the flow rule and hardening law in plasticity theory, the evolution of the damage variable d and of the radius of the damage surface r are defined by the following equations:

$$\dot{d} = \dot{\mu} H(\xi, d) \tag{2.2.9a}$$

$$\dot{r} = \dot{\mu} \tag{2.2.9b}$$

Here $\dot{\mu} \geq 0$ is the damage consistency parameter that defines damage loading/unloading conditions according to the standard Kuhn-Tucker forms:

$$\dot{\mu} \geq 0, \qquad g(\xi, r) \leq 0, \qquad \dot{\mu} g(\xi, r) = 0 \tag{2.2.10}$$

Further, the radius r is determined by the expression:

$$r = \max [r_0, \max \xi] \tag{2.2.11}$$

where max ξ denotes the maximum value of ξ over the entire time history up to the instant considered. In the event of loading, $\dot{\mu}$ is determined by the damage consistency condition; that is:

$$g(\xi, r) = \dot{g}(\xi, r) = 0 \quad \Rightarrow \quad \dot{\mu} = \dot{\xi} \tag{2.2.12}$$

For simplicity, the function $H(\xi, d)$ in Eq. (2.2.9a) is often assumed to be independent of d. H is then a function of the "measure of strain energy" ξ only. Owing to this assumption, (2.2.9) then possesses a structure analogous to that of the rate form of hyperelasticity. That is, d is purely a function of ξ_{max}:

$$d = \phi(\xi_{max}) \tag{2.2.13}$$

where ϕ is a *damage accumulation function*.

2.3. Elasto-Plastic Damage Models

When damage and plastic flow processes are considered, a free energy of the following form is considered (Simo and Ju, 1987a):

$$\Psi(\boldsymbol{\varepsilon},\boldsymbol{\sigma}^p,\mathbf{q},d) = (1-d)\Psi_0(\boldsymbol{\varepsilon}) - \boldsymbol{\varepsilon}:\boldsymbol{\sigma}^p + \Xi(\mathbf{q},\boldsymbol{\sigma}^p) \tag{2.3.1}$$

where $\mathbf{q}$ is a suitable set of internal plastic variables and $\boldsymbol{\sigma}^p$ the plastic relaxation stress tensor. The formalism for the plasticity-damage case is very similar to the hyperelasticity-damage model outlined above. In particular, Clausius-Duhem inequality, neglecting the effect of temperature, yields the stress-strain relationship:

$$\boldsymbol{\sigma} = \frac{\partial \Psi}{\partial \boldsymbol{\varepsilon}} = (1-d)\frac{\partial \Psi_0}{\partial \boldsymbol{\varepsilon}} - \boldsymbol{\sigma}^p \tag{2.3.2}$$

It can be noticed that the plastic response is characterized by standard forms of flow rule and hardening law, where the homogeneous stress $\boldsymbol{\sigma}$ is substituted by the effective stress $\bar{\boldsymbol{\sigma}}$. Rate-independent plastic response is characterized by the following equations:

$$\dot{\boldsymbol{\varepsilon}}^p = \dot{\lambda}\,\frac{\partial f}{\partial \boldsymbol{\sigma}}(\bar{\boldsymbol{\sigma}},\mathbf{q}) \qquad (\textit{associative flow rule}) \tag{2.3.3a}$$

$$\dot{\mathbf{q}} = \dot{\lambda}\,\mathbf{h}(\bar{\boldsymbol{\sigma}},\mathbf{q}) \qquad (\textit{plastic hardening law}) \tag{2.3.3b}$$

$$f(\bar{\boldsymbol{\sigma}},\mathbf{q}) \le 0 \qquad (\textit{yield condition}) \tag{2.3.3c}$$

The elasto-plastic constitutive law will now be expressed in an rate form:

$$\dot{\boldsymbol{\sigma}} = \mathbf{C}:\dot{\boldsymbol{\varepsilon}} \tag{2.3.4}$$

The the tangent moduli tensor $\mathbf{C}$ will depend on the undamaged elastic tensor C^0 as well as the damage d, the plastic flow rule and the hardening law (Simo and Ju, 1987).

In the elastic zone, the tensor of tangent moduli will be:

$$\mathbf{C} = \mathbf{C}^{el} = (1-d)\,\mathbf{C}^0 \tag{2.3.5a}$$

$\mathbf{C}^0$ is the undamaged tensor of elastic moduli. In the plastic zone the following will hold:

$$\mathbf{C} = \mathbf{C}^{el} - \mathbf{C}^{ep} \tag{2.3.5b}$$

with

$$\mathbf{C}^{ep} = (1-d)\,\frac{\mathbf{C}^0\frac{\partial f}{\partial \boldsymbol{\sigma}} \otimes \mathbf{C}^0\frac{\partial f}{\partial \boldsymbol{\sigma}}}{\mathbf{C}^0\frac{\partial f}{\partial \boldsymbol{\sigma}}\frac{\partial f}{\partial \boldsymbol{\sigma}} - \frac{\partial f}{\partial \mathbf{q}}\cdot\mathbf{h}} \tag{2.3.6}$$

Equations (2.3.5) are only approximately valid. In general, there is a history-dependent contribution that is neglected here for simplicity. The denominator in equation (2.3.6) is positive definite in all cases of practical interest.

SECTION 3: LOCAL DAMAGE VARIABLES AND PARAMETER BASED DAMAGE INDICES: ELASTIC VIBRATION OF A DAMAGED BODY

3.1. Introduction

Continuum Damage Mechanics deals with damage at a local level. An internal variable d is defined for each point of the structure under study. Since a structure is continuous, its global damage state would depend on an infinite number of parameters and the problem would not be amenable to analytical or numerical treatment. It is therefore necessary to reduce the dimensions of the problem by postulating that only a finite number of parameters are needed to define the structure's damage state. Parameter-based damage indices have been introduced as a measure of structural damage. Such indices are computed from the equivalent linear frequencies of the structure. The relationship between parameter-based indices and internal damage variables will now be investigated. The onset of elastic damage will introduce some nonlinearities in the behavior of an originally linear elastic body. However, after the damage event occurs, the body will still present a linear behavior with degraded characteristics both at the global and at the local level, as summarized in Table 3-1.

The expression for the final softening is recalled here:

$$\delta_f = 1 - \frac{\omega^2}{\omega_0^2} \tag{3.1.1}$$

Note that ω_0 is the fundamental frequency of the free vibration of the undamaged solid (undamaged natural frequency), and ω is the fundamental frequency of the free vibration of the damaged body (damaged natural frequency).

Let V be the volume occupied by a continuous body, bounded by a surface $S = S_1 \cup S_2$. Displacements are assigned on S_1 and tractions are assigned on S_2. Within the volume V, the equilibrium equations, disregarding the body forces, are:

$$\nabla \cdot \sigma = \rho \frac{d^2 u}{dt^2} \tag{3.1.2}$$

Table 3-1: Undamaged characteristic vs. damaged characteristics		
	UNDAMAGED	DAMAGED
fundamental frequency	ω_0	ω
fundamental mode shape	$\mathbf{y}_0$	$\mathbf{y} = \mathbf{y}_0 + \Delta\mathbf{y}$
strain energy density	$\Psi_0(\varepsilon)$	$(1-d)\Psi_0(\varepsilon)$
linear secant moduli	E_0, G_0	$(1-d)E_0, (1-d)G_0$

Further, assume that Eq. (3.1.2) has a harmonic solution:

$$\mathbf{u}_0(\mathbf{x},t) = \mathbf{y}_0(\mathbf{x}) \sin\omega_0 t \tag{3.1.3}$$

corresponding to the fundamental mode shape $\mathbf{y}_0(\mathbf{x})$ and the fundamental frequency ω_0. For the undamaged body, the elastic strain energy is:

$$W = \int_V \frac{1}{8}(u_{i,j}+u_{j,i})\, C^0_{ijkl}(u_{k,l}+u_{l,k})\, dV = \int_V \Psi_0(\mathbf{u}(x,t))\, dV \tag{3.1.4a}$$

where $\mathbf{C}^0$ and Ψ_0 have previously been defined in Eq. (11). In the case of harmonic oscillation (3.1.3), the kinetic energy of the body can be written as follows:

$$T = \int_V \tfrac{1}{2}\rho\dot{\mathbf{u}}\cdot\dot{\mathbf{u}}\, dV = \int_V \omega^2\, \mathbf{y}\cdot\mathbf{y} \cos^2\omega t\, dV = \int_V \omega^2\, T_0[\mathbf{y}(x)] \cos^2\omega t\, dV \tag{3.1.4b}$$

The scalar quantity $T_0 \equiv \frac{1}{2}\rho\, \mathbf{y}\cdot\mathbf{y}$ is a measure of the density of the kinetic energy.

An expression for the undamaged fundamental frequency can be obtained by applying Hamilton's principle. That is, for any pair of instants t_1 and t_2 the integral of the sum of the first variations of the kinetic and potential energy must be stationary:

$$\int_{t_1}^{t_2} \delta\,(T+W)\, dt = 0 \tag{3.1.5}$$

The resulting undamaged fundamental frequency is:

$$\omega_0^2 = \frac{\int_V \Psi_0(\mathbf{y}_0)\, dV}{\int_V T_0(\mathbf{y}_0)\, dV} \tag{3.1.6}$$

It is noted that in Eq. (3.1.6) and in what follows, $\Psi_0(\mathbf{y})$ and $T_0(\mathbf{y}_0)$ should be read as $\Psi_0[\mathbf{y}(\mathbf{x})]$ and $T_0[\mathbf{y}(\mathbf{x})]$ respectively.

It can be shown (Rayleigh, 1894) that the first variation of the ratio (3.1.6) vanishes at $\omega^2 = \omega_0^2$:

$$\left[\delta\omega^2\right]_{\omega=\omega_0} = \frac{-\delta(T+W)}{\int_V T_0(\mathbf{y}_0)\, dV} = 0 \tag{3.1.7}$$

It can also be proven that the energy ratio (3.1.6) attains a minimum when $\omega^2 = \omega_0^2$. In the above equations, the variational notation "δ" should not be confused with the symbols used to indicate damage indices.

If a deformed mode shape $\mathbf{y} = \mathbf{y}_0 + \Delta\mathbf{y}$ is considered, the variation of the energy ratio (3.1.6) will be of the second order with respect to $|\Delta\mathbf{y}|$ as $\Delta\mathbf{y}\to 0$:

$$\frac{\int_V \Psi_0(\mathbf{y})\, dV}{\int_V T_0(\mathbf{y})\, dV} = \omega_0^2 + \omega_0^2\, \varepsilon^2(\Delta \mathbf{y}) \tag{3.1.8}$$

where ε^2 is a positive definite function of the variation $\Delta \mathbf{y}$ of the mode shape. From (3.1.7) it follows that, as $\Delta \mathbf{y} \to 0$, $\varepsilon^2(\Delta \mathbf{y}) \approx |\Delta \mathbf{y}|^2$.

In vibrational analysis, it is customary to refer to the ratio $\frac{\int_V \Psi_0(\mathbf{y}) dV}{\int_V T_0(\mathbf{y}) dV}$ as the Rayleigh ratio $R(\mathbf{y})$. Using this notation the function $\varepsilon^2(\Delta \mathbf{y})$ can be written as:

$$\varepsilon^2(\Delta \mathbf{y}) = \frac{R(\mathbf{y}_0 + \Delta \mathbf{y})}{R(\mathbf{y}_0)} - 1 \tag{3.1.9}$$

3.2. Relation between Final Softening and Global Stiffness Degradation

In the case of elastic damage, the elastic strain energy decreases by a factor $(1-d(\mathbf{x}))$. The damaged body will have a new frequency of oscillation $\omega \le \omega_0$, corresponding to a damaged mode shape $\mathbf{y} = \mathbf{y}_0 + \Delta \mathbf{y}$. It should be pointed out that, even though the damaged frequency ω can be much lower than the original frequency ω_0, the damaged mode shape will *not* usually be very different from the original one. The undamaged strain energy $\Psi_0(\mathbf{y})$ corresponding to the damaged mode shape can be used as a weighting function in the definition of an *"average damage"* d_{av}:

$$d_{av} \equiv \frac{\int_V d(\mathbf{x}) \Psi_0(\mathbf{y}) dV}{\int_V \Psi_0(\mathbf{y}) dV} \tag{3.2.1}$$

The following result can now be proven:

Proposition 3.I

The following relationship holds between the average damage d_{av} and the final softening δ_f:

$$d_{av} = \delta_f + (1-d_{av})\, \varepsilon^2(\Delta \mathbf{y}) \tag{3.2.2}$$

Proof

The Hamilton's principle can be used to compute the damaged frequency:

$$\omega^2 = \frac{\int_V (1-d(\mathbf{x}))\,\Psi_0(\mathbf{y})\,dV}{\int_V T_0(\mathbf{y})\,dV} = \frac{\int_V \Psi_0(\mathbf{y})\,dV}{\int_V T_0(\mathbf{y})\,dV} - \frac{\int_V d(\mathbf{x})\,\Psi_0(\mathbf{y})\,dV}{\int_V T_0(\mathbf{y})\,dV} \tag{3.2.3}$$

By substituting Eq. (3.1.8) into (3.2.3) we obtain:

$$\omega^2 = \omega_0^2 - \frac{\int_V d(\mathbf{x})\,\Psi_0(\mathbf{y})\,dV}{\int_V T_0(\mathbf{y})\,dV} + \omega_0^2\varepsilon^2(\Delta\mathbf{y}) \tag{3.2.4}$$

Therefore:

$$\delta_f = 1 - \frac{\omega^2}{\omega_0^2} = \frac{\int_V d(\mathbf{x})\,\Psi_0(\mathbf{y})\,dV}{\omega_0^2 \int_V T_0(\mathbf{y})\,dV} - \varepsilon^2(\Delta\mathbf{y}) \tag{3.2.5}$$

Multiplying numerator and denominator on the right hand side by $\int_V \Psi_0(\mathbf{y})\,dV$, recalling (3.1.8) and (3.2.1) and neglecting terms of order higher than 2 with respect to $|\Delta\mathbf{y}|$, the final result is obtained:

$$\delta_f = d_{av} - (1 - d_{av})\,\varepsilon^2 \tag{3.2.6}$$

The parameter based damage index (3.1.1) will therefore be approximately equal to a weighted average of the local damage variable when the mode shape does not change significantly after damage. In general the approximation will be of the second order as the two mode shapes get close to each other. The average damage d_{av} defined in Eq. (3.2.1) has particular significance for earthquake engineers when the first (fundamental) mode of vibration is considered.

3.3. Application of Proposition 3.I: the Final Softening as a Measure of Global Damage

Proposition 3.I establishes the relationship between the local stiffness degradation and global damage indices based on vibrational parameters. In particular, from (38) we acquire:

$$d_{av} = \delta_f + (1-d_{av})\,\varepsilon^2(\Delta \mathbf{y}) \tag{3.3.1}$$

Before considering applications of the final softening to experimental data, it is perhaps interesting to consider a particularly simple case. Let us consider a two degrees of freedom linear system (Figure 3.1). For simplicity it is assumed that the two interstory spring elements have an equal stiffness k_0 and the two lumped masses have equal value m. A damage event will result in a degradation of the interstory stiffnesses, with the degraded values being $(1-d_1)k_0$ and $(1-d_2)k_0$. The undamaged frequency of the first mode of vibration (fundamental frequency) is given by:

$$\omega_0^2 = \frac{k_1+2k_2-(k_1^2+4k_2^2)^{\frac{1}{2}}}{2m} = \frac{k_0}{m}\,\frac{3-\sqrt{5}}{2} \tag{3.3.2}$$

As for the first undamaged mode shape, it will depend only on one parameter. If the amplitude y_2 of the oscillation of the top mass is taken as one, then for the first degree of freedom (bottom mass) we have:

$$y_1^{(0)} = \frac{\frac{k_2}{m}}{\frac{k_1}{m}+\frac{k_2}{m}-\omega_0^2} = \frac{1}{2-\frac{3-\sqrt{5}}{2}} \tag{3.3.3}$$

After damage, the frequency and the mode shape will change, respectively, to:

$$\omega^2 = \frac{k_0}{m}\,\frac{(1-d_1)+2(1-d_2)-((1-d_1)^2+4(1-d_2)^2)^{\frac{1}{2}}}{2} \tag{3.3.4}$$

$$y_1 = \frac{(1-d_1)\frac{k_0}{m}}{(1-d_1)\,\frac{k_0}{m}+(1-d_2)\,\frac{k_0}{m}-\omega^2} \tag{3.3.5}$$

A damage event is therefore described by a pair of values $(d_1,d_2) \in [0,1]\times[0,1]$ for the

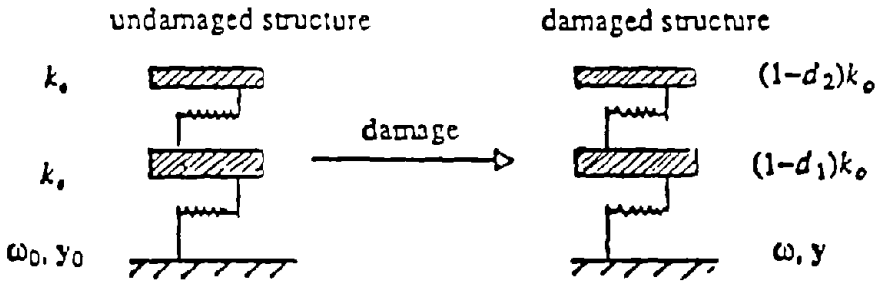

Figure 3.1: Simulation of Damage to a 2-DOF Linear System

damage at two stories. The ability of the final softening to measure global stiffness degradation can now be assessed. Figure 3.2 shows a plot of the level curves of the error function $(d_{av}-\delta_f)$. As predicted by Eq. (3.2.2), the error is always positive and becomes very small in the vicinity of the diagonal $d_1=d_2$, due to the second order nature of the function $\varepsilon^2(\Delta y)$. In particular, the error vanishes when $d_1=d_2$. When damage is equally spread throughout the structure, in fact, the mode shape is not modified after damage. In this case, the value of the final softening coincides with that of the story damage. It is also interesting to notice that, as long as the damage of the first story d_1 is greater than that of the second story d_2, the error is very small. The only region where the error is significant corresponds to high values of d_2 coupled with low values of d_1.

The relationship between global damage indices and local damage variables obtained above can be used in the analysis of seismic response data. A particularly interesting program of shaking table experiments was carried out at the University of Illinois at Urbana-Champagne (UIUC) by Sozen and his associates (Healey and Sozen, 1978; Abrams and Sozen, 1979; Cecen, 1979; Sozen, 1981). The experiments analyzed here come from a population of seven ten-story, 1/10th-scale structures, representative of a wide variety of reinforced concrete design techniques.

Each structure was tested at the University of Illinois Earthquake Simulator. Test runs of a given structure included repetitions of the following sequence:

(1) Free vibration test to determine low-amplitude natural frequencies.

(2) Earthquake simulation.

(3) Recording of any observable signs of damage.

The results of the analysis of this series of shaking table experiments have been presented by DiPasquale and Çakmak (1988). No information was available about the floor stiffness degradation subsequent to each test run. However, the average story damage can be computed from the maximum story drift, as reported by the experimenters, using a simple continuum damage model proposed by Ju et al. (1989). Although the structures experienced significant nonlinearities, the permanent deformation observed at the end of most runs were very small. The use of an elastic-damage model is thus justified. The local value of damage depends on the maximum

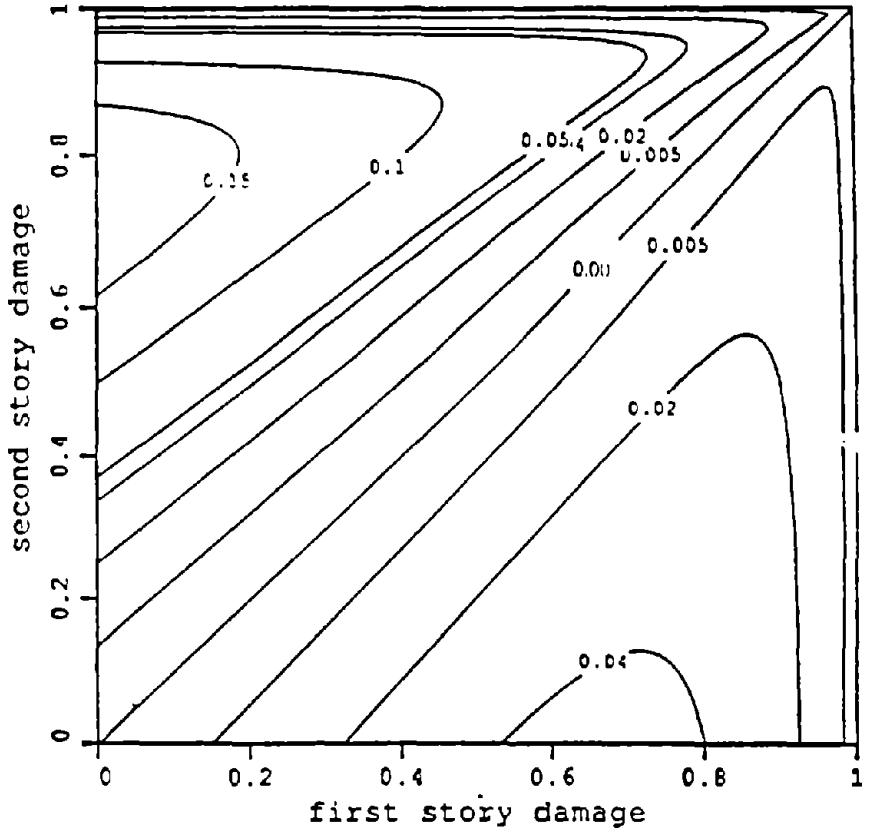

Figure 3.2: Level Curves for the Error Function ($d_{av} - \delta_f$)

measure of strain energy ξ_{max}, as indicated in Eqs. (17) and (21):

$$\xi_{max} = \max[(2\Psi_0(\varepsilon))^{\frac{1}{2}}] \tag{3.3.6}$$

The dependence of the d on ξ_{max} is given by a damage accumulation law (Ju et al., 1989):

$$d(\xi_{max}) = \begin{cases} 0 & \xi_{max} < \xi_0 \\ 1 - \dfrac{(1-A)\xi_0}{\xi_{max}} - A\exp[B(\xi_0 - \xi_{max})] & \xi_{max} \geq \xi_0 \end{cases} \tag{3.3.7}$$

where A and B are damage growth parameters, while ξ_0 is a damage energy threshold. All three constants are characteristic of the material.

If the maximum story drift γ_i at the i-th level is known, it is possible to compute the average maximum strain energy $\Psi_{0,i}$; i.e. the average strain energy of the column at the instant of maximum deformation. Consequently, the average measure of strain energy ξ_i can be obtained. Under the assumption that the girders are rigid (verified in practice for the case of the UIUC structures), $\Psi_{0,i}$ is given by:

$$\Psi_{0,i} = \frac{Eb^2}{h^2}\gamma_i^2 \tag{3.3.8}$$

where E is the Young's modulus of concrete ($E = 24000\,MPa$) while b and h are respectively the width and the height of the column (the actual values, assumed constant for all the stories, are $b = 0.051m$ and $h = 0.229m$).

Therefore the average damage d_i at each floor can be computed from Eq. (3.3.7). Finally, the expression for the structure's average damage d_{av} in Proposition 3.I can be approximated by:

$$d_{av} \approx \frac{\sum d_i \Psi_{0,i}}{\sum \Psi_{0,i}} = \frac{\sum d_i \gamma_i^2}{\sum \gamma_i^2} \tag{3.3.9}$$

We have assumed that the structure was vibrating mainly in the (damaged) first mode shape. It is emphasized that this assumption is consistent with the experimental report.

In Figure 3.3, the final softening δ_f and the average damage d_{av} are compared. The constants used in Eq. (3.3.7), typical of concrete materials, are (Ju et al., 1989):

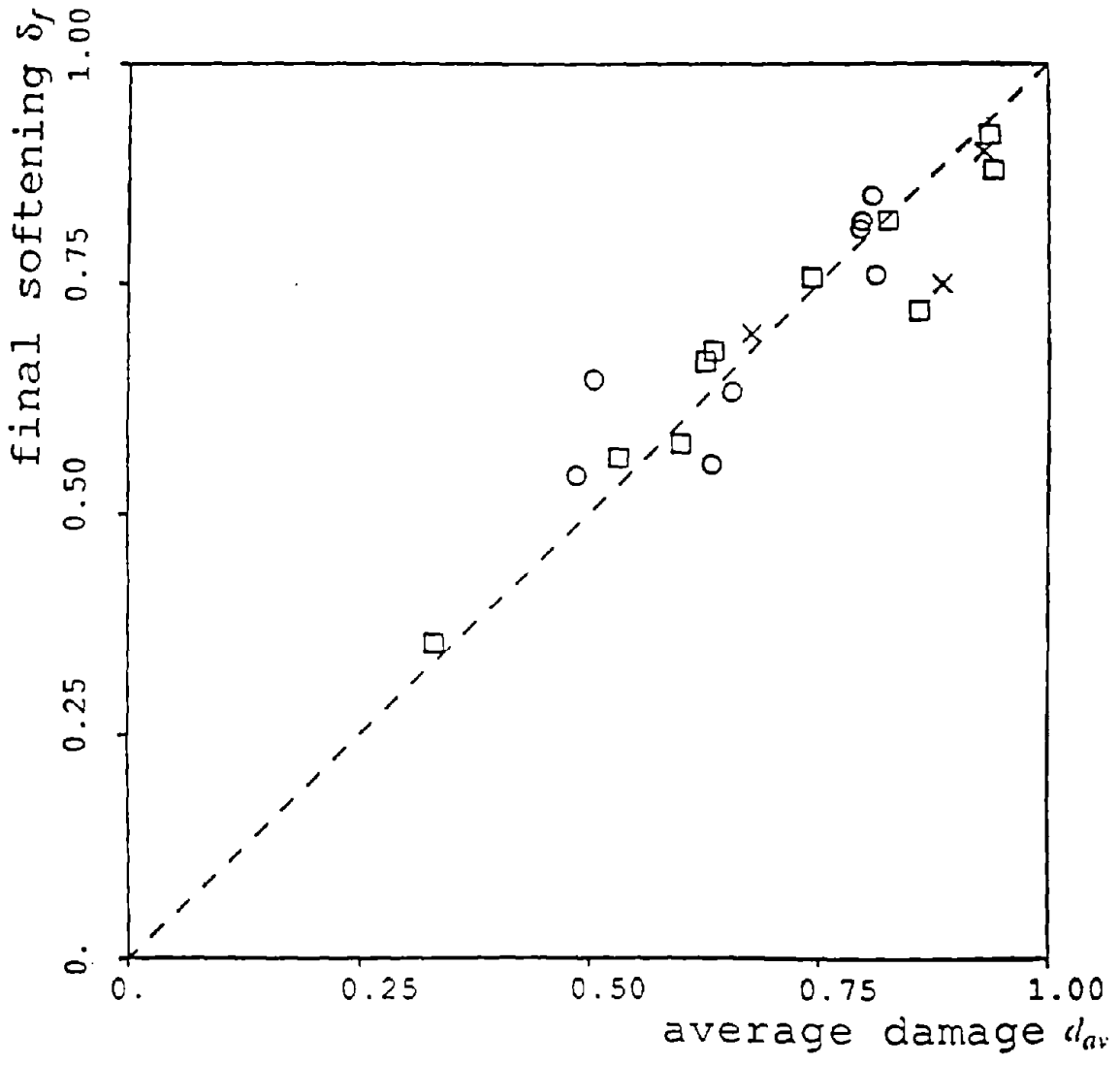

Figure 3.3: Comparison between δ_f and d_{av}
for the UIUC Database

A	0.65
B	1.50
ξ_0	303 kPa

It is clear that the agreement between the predicted and the measured global stiffness degradation is very good. Proposition 3.I is thus confirmed by the analysis of experimental data.

SECTION 4: GLOBAL DAMAGE INDICES AND PLASTIC DEFORMATION

4.1. Introduction

It is well known that a structure that experiences an earthquake of damaging intensity will show a nonlinear behavior. Permanent or plastic deformation will usually take place. Many researchers have correlated plastic deformation (or equivalently ductility) with structural damage. When nonlinear behavior is present no natural frequencies can be defined. Nevertheless an equivalent linear system can be defined and its natural frequencies ω_{eq} computed. The process of defining an equivalent linear system and computing its eigenvalues is termed equivalent linearization. In general the parameters of the equivalent linear system are chosen so to minimize some functionals of the response of the system investigated and of the equivalent linear system. When no noise is present, analytical equivalent linearization techniques are used, such as the energy balance criterion, the harmonic balance criterion, or the error-in-the-equation criterion (Chaughey, 1963). In the presence of noise it is necessary to use statistical techniques, such as the error-in-the-output criterion or the maximum likelihood criterion. As nonlinearities produce a decrease in the equivalent fundamental frequency of a structure, parameter-based global damage indices reflect the development of plastic deformation. In the following, global damage indices are related to local plastic strain. The treatment presented here is based on analytical techniques of equivalent linearization, namely on the error-in-the-equation criterion. The results of equivalent linearization based on statistical techniques would converge to that, obtained using the error-in-the-equation criterion, when the noise is negligible (Eychoff, 1974). In the analytical treatment given below the fundamental frequency, which is the inverse of the fundamental period, is considered. Different values of the fundamental frequency will correspond to different states of the structure, as summarized here:

undamaged linear structure	ω_0
damaged linear structure	ω
damaged nonlinear structure	ω_{eq}

4.2. Relation between Plastic Softening and Plastic Deformation

Consider now a continuum that occupies a volume V bounded by a surface $S = S_1 \cup S_2$. It is assumed that displacement are assigned on S_1 and tractions are assigned on S_2. Let S_2 be traction free, except for a point where a concentrated load $F(t)$ is applied. As $F(t)$ is increased, plastic deformation will take place in a portion $V_p \subseteq V$ of the body. Let the damaged elasto-plastic behavior of the body be described by equations (2.3.3) through (2.3.5).

Let $x(t)$ be the displacement of the point of application of F in the direction of the force. The application of $F(t)$ generates a displacement field $\mathbf{u}$, a strain field $\boldsymbol{\varepsilon}$ and a stress field $\boldsymbol{\sigma}$, all function of position and time. The goal is now to find a linear single degree of freedom system that is equivalent to the nonlinear continuum in the error-in-the-equation sense. A nonlinear single degree of freedom approximation is given by a nonlinear differential equation:

$$m\ddot{x} + f(x,t) = F(t) \tag{4.2.1}$$

where f is the static restoring force corresponding to a displacement x at time t and m is an equivalent mass.

The linear equivalent of (4.2.1) is:

$$\ddot{x} + \omega_{eq}^2 x = \frac{F(t)}{m} \tag{4.2.2}$$

In order to compute ω_{eq}^2 equation (4.2.2) is subtracted from (4.2.1). The difference is squared and integrated over the interval $(0,T)$ considered. The error is:

$$\varepsilon^2 = \int_0^T (f(x,t) - \omega_{eq}^2)^2 dt \tag{4.2.3}$$

The error ε^2 is then minimized with respect to ω_{eq}^2 to obtain:

$$\omega_{eq}^2 = \frac{\int_0^T x f(x,t) dt}{m \int_0^T x^2 dt} \tag{4.2.4}$$

If the equivalent frequency ω_{eq} is compared to the frequency of the linear oscillations of the damaged body ω a damage index, called plastic softening δ_p can be defined:

$$\delta_p = 1 - \frac{\omega_{eq}^2}{\omega^2} \tag{4.2.5}$$

Proposition 4.I

The plastic softening δ_p is equal to an average of the plastic strain over the volume V and over the interval $(0,T)$.

Proof

Corresponding to a value f of the restoring force at time t, let the displacement field be $\mathbf{u}$, with a strain field $\boldsymbol{\varepsilon}$ and a stress field $\boldsymbol{\sigma}$. Consider a field of virtual displacements $\delta\mathbf{u}, \delta\boldsymbol{\varepsilon}$. At the point where F is applied, the virtual displacement is δx. There will exist a particular field of virtual displacements such that

$$\delta\boldsymbol{\sigma} = \mathbf{C}:\delta\boldsymbol{\varepsilon}$$

is a virtual stress field. The tensor $\mathbf{C}$ is the tangent modulus of equations (2.3.4). In the elastic zone, the tangent moduli tensor will be:

$$\mathbf{C} = \mathbf{C}^{el} = (1-d)\,\mathbf{C}^0$$

$\mathbf{C}^0$ is the undamaged tensor of elastic moduli. In the plastic zone the following will hold:

$$\mathbf{C} = \mathbf{C}^{el} - \mathbf{C}^{ep}$$

with $\mathbf{C}^{ep}$ given by (2.3.5).

An increment δf of the restoring stress will correspond to the virtual force field $\delta\boldsymbol{\sigma}$.

An application of the theorem of second order virtual work yields:

$$\delta x\ \delta f = \int_V \delta\boldsymbol{\varepsilon}:\delta\boldsymbol{\sigma}\, dV = \int_V \delta\boldsymbol{\varepsilon}:\mathbf{C}^{el}:\delta\boldsymbol{\varepsilon}\, dV - \int_{V_p} \delta\boldsymbol{\varepsilon}:\mathbf{C}^{ep}:\delta\boldsymbol{\varepsilon}\, dV \tag{4.2.6}$$

From the associative flow rule (2.3.3b) it can be proved that the following relationship holds between $\delta\boldsymbol{\varepsilon}$ and the increment $\delta\boldsymbol{\varepsilon}^p$ of the permanent deformation:

$$\mathbf{C}^{el}:\delta\boldsymbol{\varepsilon}^p = \mathbf{C}^{ep}:\delta\boldsymbol{\varepsilon} \tag{4.2.7}$$

Substituting in (4.2.6) an expression for δf is obtained:

$$\delta_f = \frac{1}{\delta x}\int_V \delta\boldsymbol{\varepsilon}:\mathbf{C}^{el}:\delta\boldsymbol{\varepsilon}\, dV - \frac{1}{\delta x}\int_V \delta\boldsymbol{\varepsilon}:\mathbf{C}^{el}:\delta\boldsymbol{\varepsilon}^p \tag{4.2.8}$$

Equation (4.2.4) can now be rewritten as:

$$\omega_{eq}^2 = \frac{\int_0^T x f_{\cdot}(x,t)dt}{m\int_0^T x^2 dt} = \frac{\int_0^T x dt \int_0^t df}{m\int_0^T x^2 dt} \tag{4.2.9}$$

Substituting now equation (4.2.8) into (4.2.9) an expression for the equivalent frequency in terms of the history of plastic deformation is obtained:

$$\omega_{eq}^2 = \frac{\int_0^T x dt \int_0^t \frac{1}{\delta x}\int_V \delta\varepsilon : C^{el} : \delta\varepsilon \, dV}{m\int_0^T x^2 dt} - \frac{\int_0^T x dt \int_0^t \frac{1}{\delta x}\int_{V_p} \delta\varepsilon : C^{el} : \delta\varepsilon^p \, dV}{m\int_0^T x^2 dt} \tag{4.2.10}$$

The first term on the right hand side of the equation above represents the equivalent frequency corresponding to the case where no plastic deformation takes place, and it is therefore equal to the damaged frequency of linear oscillations ω^2. Dividing through by ω^2 and rearranging, the final expression is obtained:

$$\delta_p = 1 - \frac{\omega_{eq}^2}{\omega^2} = \frac{\int_0^T x dt \int_0^t \frac{1}{\delta x}\int_{V_p} \varepsilon : C^{el} : \delta\varepsilon^p \, dV}{m\,\omega^2 \int_0^T x^2 dt} \tag{4.2.11}$$

This proves Proposition 4.I.

Thus when the equivalent frequency ω_{eq} is compared with the frequency ω of the linear vibrations of the damaged body the result, which has been called plastic softening δ_p, is an average in space and in time of the plastic strain. Recalling equation (2.3.5) for C^{ep}, it should be pointed out that the plastic softening (4.2.11) depends on the distribution and on the evolution of damage as well as on that of the plastic strain. This should be expected as plasticity and damage are coupled even in simplified models like the one described in Section 7.2 .

4.3. Application of Proposition 4.I: Case of a Nonlinear Shear Building

Equation (4.2.11) may look unsuitable for practical application. The analysis of simple structural systems will provide a physical interpretation. The first case analyzed is that of a single degree of freedom nonlinear system with elastic unloading. It will be assumed that damage and subsequent stiffness degradation have already taken place. The degraded linear characteristics of the structural elements is thus used

as reference and no coupling exists between plasticity and damage. The restoring force f can be split into an elastic component f_e and a plastic relaxation f_p (Figure 4.1):

$$f = f_e - f_p = k(x - x_p) \tag{4.3.1}$$

where k is the stiffness that the system exhibits in the linear regime (assumed equal to that of the elastic unloading), while x and x_p are respectively the total and the plastic displacement.

The equivalent stiffness is obtained multiplying (4.2.4) by m:

$$k_{eq} = \frac{\int_0^T x f(x,t)dt}{\int_0^T x^2 dt} = \frac{k\int_0^T x^2 dt}{\int_0^T x^2 dt} - \frac{k\int_0^T x x_p dt}{\int_0^T x^2 dt} = k - \frac{k\int_0^T x x_p dt}{\int_0^T x^2 dt} \tag{4.3.2}$$

The plastic index δ_p is therefore:

$$\delta_p = 1 - \frac{\omega_{eq}^2}{\omega^2} = 1 - \frac{k_{eq}}{k} = \frac{\int_0^T x x_p dt}{\int_0^T x^2 dt} = \frac{<x, x_p>}{<x, x>} \tag{4.3.3}$$

The plastic softening δ_p is therefore a measure of the correlation between the total and the plastic deformation. As an example, an elastic-perfectly-plastic system can be considered. If the time history of the strain is a sinusoidal wave $x = x_0 \cos \eta t$, the total and the plastic strain can be drawn as in Figure (4.2). It can be seen that for small values of the plastic strain the plastic softening will be negligible. As x_0 increases and more plastic deformation appears the time history of x and of x_p will tend to coincide and the plastic softening will approach one. For any analytical model of structural behavior δ_p can be written as a function of the plastic strain developed. It can therefore be used as a measure of ductility.

If a multi degree of freedom structure is analyzed, the procedure of equivalent linearization can be thought of as substituting each nonlinear element with an equivalent linear spring of stiffness given by (4.3.2). Under the assumption that the modal shape remains unchanged, ω_{eq}^2 can be computed using Rayleigh's method. Consider for example the case of a n-storied nonlinear shear building. If y_i is the displacement of the ith story in the damaged fundamental mode shape and h_i is the height of the story, the story drift at the ith level is:

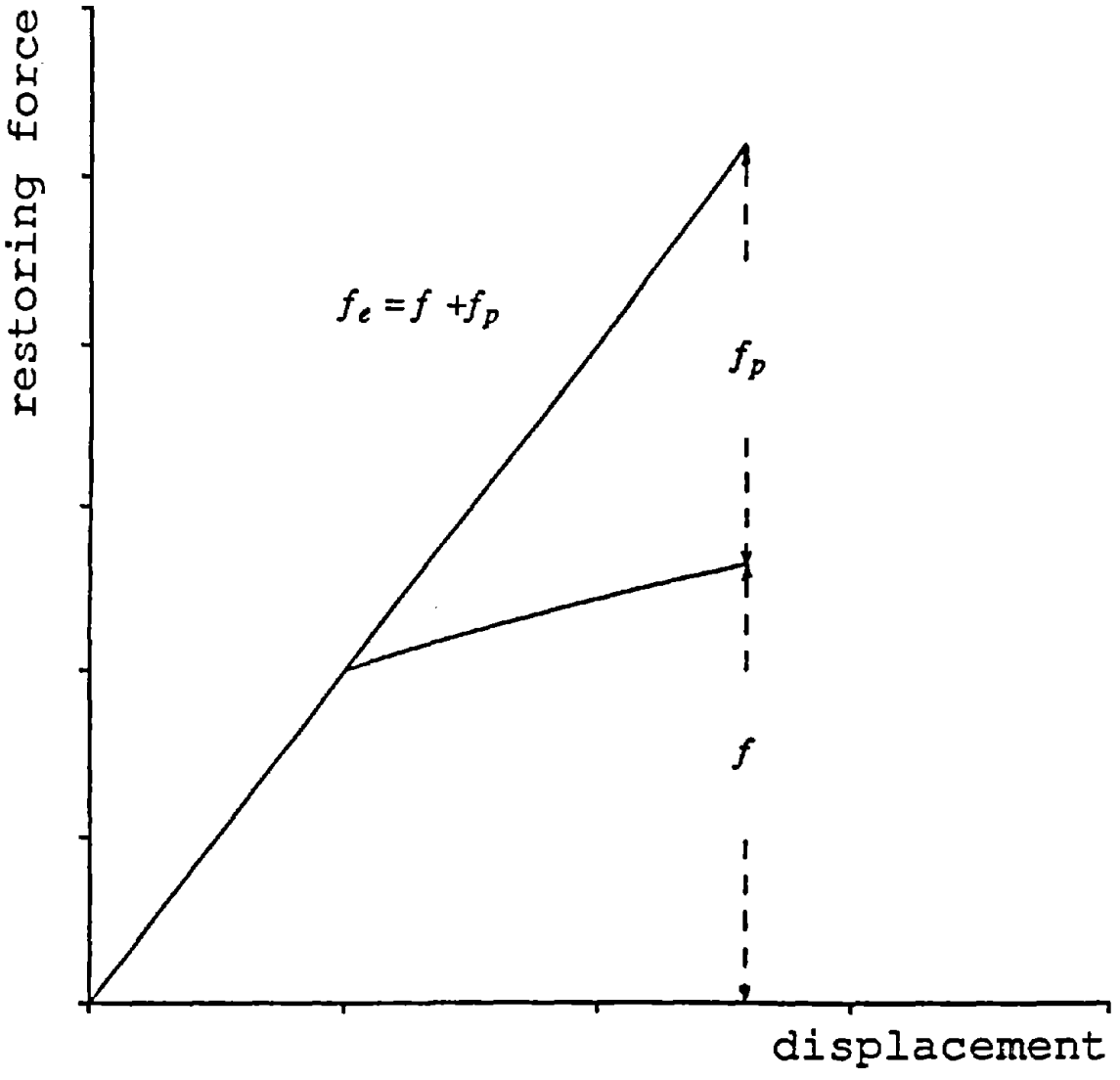

Figure 4.1: Stress Split for a Nonlinear SDOF System

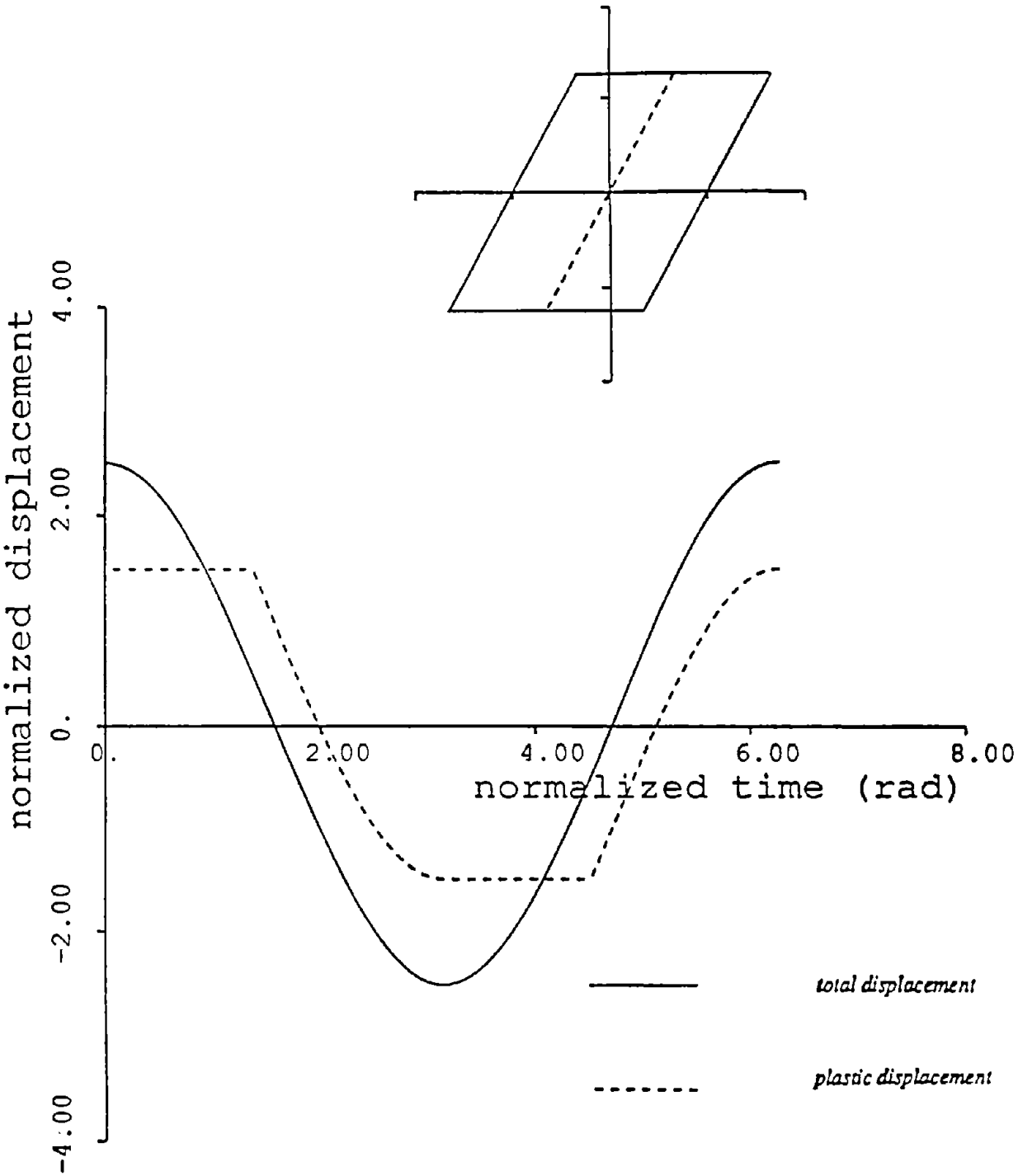

Figure 4.2: Total and Plastic Displacement for an Elasto-Plastic SDOF Oscillator

$$\gamma_i = \frac{y_i - y_{i-1}}{h_i} \tag{4.3.4}$$

and the ratio of ω_{eq}^2 over ω^2 is:

$$\frac{\omega_{eq}^2}{\omega^2} = \frac{\sum_{i=1}^{n} k_{eq,i}\gamma_i^2}{\sum_{i=1}^{n} k_i \gamma_i^2} \tag{4.3.5}$$

Recalling that (equation (4.3.2))

$$k_{eq,i} = k_i \left[1 - (\frac{<\gamma,\gamma_p>}{<\gamma,\gamma>})_i\right] \tag{4.3.6}$$

the following expression for the plastic softening is obtained:

$$\delta_p = 1 - \frac{\omega_{eq}^2}{\omega^2} = \frac{\sum_{i=1}^{n} (\frac{<\gamma,\gamma_p>}{<\gamma,\gamma>})_i k_i \gamma_i^2}{\sum_{i=1}^{n} k_i \gamma_i^2} \tag{4.3.7}$$

The plastic softening is therefore equal to the weighted average of the ratio $\frac{<\gamma,\gamma_p>}{<\gamma,\gamma>}$ at each floor, hence of the ductility developed at each level during the interval considered. The weights that relate the local values of ductility to the global index represent the elastic strain energy stored in the damaged body.

The similarity between equation (4.3.7) and equation (3.3.9), where the final softening is defined as an average of the local stiffness degradation, should be pointed out.

SECTION 5: DEFINITION OF FRAGILITY CURVES BASED ON GLOBAL DAMAGE INDICES

5.1. Analysis of Seismic Structural Response

Post earthquake damage assessment involves decisions regarding the future of the building, such as whether the building is safe or needs some actions, ranging from cosmetic repairs to demolition. In a model for the analysis of seismic damage these decision will correspond to different limit states. The decision to undertake a particular action is then equivalent to assessing whether the corresponding limit state has been trespassed or not.

Parameter-based global damage indices have been introduced above as a measure of seismic structural damage. It has been shown that the maximum softening, as defined in equation (2.2.3), repeated below:

$$\delta_M = 1 - \frac{(T_0)_{initial}}{(T_0)_{\max}} \tag{5.1.1}$$

depends on the combined effect of stiffness degradation and plastic deformations.

In order to use the maximum softening to measure global damage, a quantitative relationship must be established between the numerical value of the index, as obtained from strong motion records, and engineering features of damage, as reported by post earthquake inspection and analysis.

Seismic response data from damaged structures must thus be analyzed. Unfortunately, there are very few records from buildings that have been damaged during an earthquake. In order to find a sufficient number of structures, it is necessary to resort to seismic simulations on shaking tables. Such experiments are particularly useful for model validation, because of the following reasons:

(a) The structural models tested are usually a physical realization of an engineer's concept. Most structures analyzed in the following are designed and built so that their behavior is as close as possible to that of a moment resisting frame, sometimes in parallel with other structural elements such as a shear wall. Their response is thus very close to the analytical predictions. Furthermore, in most

cases lateral and torsional motion are prevented. The only motion possible is then parallel to the direction of the excitation. This reduces the number of degrees of freedom and simplifies the damage analysis.

(b) The structural models are extensively instrumented. Consequently it is possible to compare the performances of the method to be validated with the performances of other methods.

(c) Each structural model is used for several simulations with different levels of earthquake intensity, thus providing a large amount of data from a single structure.

5.2. Description of the Test Structures

A particularly interesting program of shaking table experiments has been realized at the University of Illinois at Urbana-Champagne (UIUC) by Sozen and his associates (Healey and Sozen, 1978, Abrams and Sozen, 1979, Cecen, 1979, Sozen, 1981). The experiments analyzed here come from a population of seven structures (Table 5-1), which may be considered grouped into two series. Each one of the first group of three test structures was made up of two ten-storied frames working in parallel, with the story weights positioned between. Test structures H1 and H2 had a uniform distribution of story heights. The first and top story for the structure MF1 were taller than the other stories. Cross-sectional dimensions of the frame elements were the same for all four test structures. The second group of test structures (FW1, FW2, FW3 and FW4) comprised three elements, two ten-storied frames working in parallel with a wall. For all test structures, the story mass weighed approximately 4.5 kN.

Each structure was tested at the University of Illinois Earthquake Simulator. Test runs of a given structure included repetitions of the following sequence:

(1) Free vibration test to determine low-amplitude natural frequencies.

(2) Earthquake simulation.

(3) Recording of any observable signs of damage such as cracking and spalling of concrete.

TABLE 5-1: SHAKING TABLE EXPERIMENTS AT UIUC					
model	authors	type of structure	earthquake excitation	undamaged first mode frequency (Hz)	total number of runs
MF1	Healey and Sozen (1978)	10-story, 3-bay double frame tall first story	El Centro (1940)	3.7	3
FW1	Abrams and Sozen (1979)	10-story, 3-bay double frame + wall heavily reinforced wall	El Centro (1940)	4.3	3
FW2	"	10-story, 3-bay double frame + wall lightly reinforced wall	El Centro (1940)	4.5	3
FW3	"	10-story, 3-bay double frame + wall lightly reinforced wall	Taft (1952)	4.0	3
FW4	"	10-story, 3-bay double frame + wall heavily reinforced wall	Taft (1952)	5.2	3
H1	Cecen and Sozen (1979)	10-story, 3-bay double frame weak beams	El Centro (1940)	2.2	3
H2	Cecen and Sozen (1979)	10-story, 3-bay double frame weak beam design	El Centro (1940)	2.7	7

This sequence was repeated with the intensity of the earthquake simulation being increased in successive sequences. For all but one (H2) structure, the first earthquake simulation represented the "design" level.

The natural frequency of a structure's linear oscillations can be estimated from the strong motion records. In the case of real-world buildings it must be assumed that no prior information about the structure is available and that the undamaged natural frequency must be estimated from the strong motion records. In Table 5-2 the fundamental frequencies estimated by the experimenters from free vibration tests are compared with those estimated from strong motion records. The general trend in both cases is toward a decrease in the fundamental frequency after earthquake simulation tests and subsequent damage. The frequencies estimated from strong motion records are lower than those estimated from free vibration tests, with the exception of the FW structures. This is due to the different amplitude of the oscillations of the structure in the two cases. Nonlinearities do not appear abruptly in structural behavior. A rather smooth change in the response can be observed as the amplitude of the oscillation increases. This accounts, for instance, for the difference that is found between the frequencies estimated from forced and from ambient vibration measurements. The values of the initial fundamental frequencies estimated for the FW structures are close to the values that the experimenters had computed analytically (Sozen,1981).

5.3. Practical Analysis of Strong Motion Records

In order to estimate the equivalent linear parameters of a structure, records from the basement and from some upper level are needed. The basement record is used as input to a numerical model that is equivalent to the original structure in the Maximum Likelihood sense (DiPasquale and Cakmak, 1987). As the actual structure is nonlinear, the equivalent linear model must be time variant. Therefore, the interval of duration of the earthquake is divided into segments (time windows) of appropriate length, and the parameter estimation is performed separately for each of these windows. The analysis of the UIUC database has been described in detail in a previous report (DiPasquale and Cakmak, 1988). As an example, Figure 5.1 shows, for the structure FW1, run 1, the acceleration records analyzed and the corresponding evolution of the softening of the structure, defined as

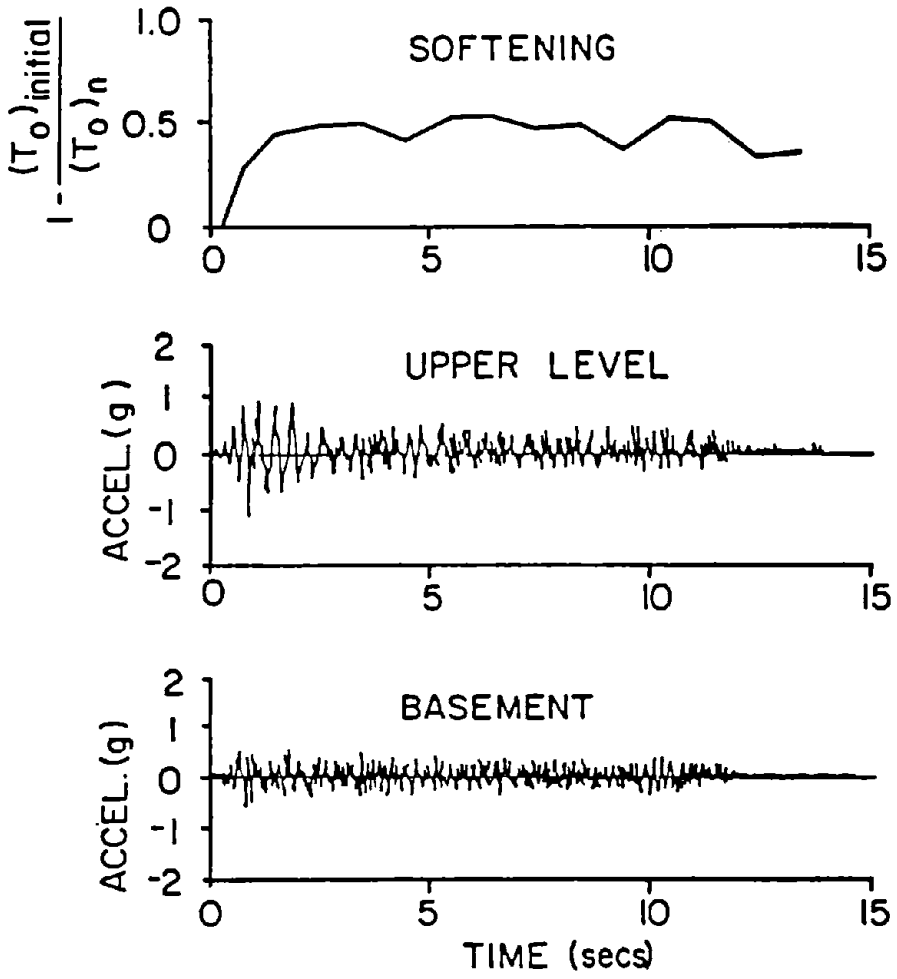

Figure 5.1: Acceleration Records and Evolution of Softening for the Structure FW1, run 1

TABLE 5-2: FUNDAMENTAL FREQUENCY (HZ) AFTER TEST RUNS			
structure	run	frequency (free vibrations)	frequency (earthquake records)
MF1	initial	3.2	3.7
MF1	1	2.9	2.2
MF1	2	2.3	1.9
MF1	3	1.9	1.2
FW1	initial	3.4	4.3
FW1	1	3.7	2.7
FW1	2	3.1	1.9
FW2	3	2.9	1.9
FW2	initial	3.3	4.5
FW2	1	3.2	3.0
FW2	2	3.1	2.0
FW2	3	nr[1]	1.8
FW3	initial	3.2	4.0
FW3	1	3.3	2.7
FW3	2	2.7	2.4
FW3	3	2.7	2.4
FW4	initial	3.2	5.2
FW4	1	3.0	3.1
FW4	2	2.8	2.1
FW4	3	2.2	1.9
H1	initial	3.0	2.2
H1	1	2.2	1.3
H1	2	1.8	0.91
H1	3	nr[1]	0.61
H2	initial	4.4	2.7
H2	1	3.3	2.2
H2	2	2.6	1.8
H2	3	2.3	1.8
H2	4	2.3	1.6
H2	5	2.0	1.4
H2	6	1.9	1.3
H2	7	nr[1]	0.9

[1] not reported.

$$1 - \frac{(T_0)_{initial}}{(T_0)_i} \tag{5.3.1}$$

where the subscript i indicates the ith window considered, and $(T_0)_i$ the respective equivalent fundamental period estimated.

The analysis of each window can be divided into two phases. First the order of the model, i.e., the number of modes whose parameters are estimated, is determined (model identification). Then the parameters are estimated using maximum likelihood techniques. If the effect of the input noise is neglected, the estimation of the modal parameters using the Maximum Likelihood criterion reduces to matching the recorded acceleration of the upper floor with the output of the modal model considered. Experience shows that one-mode models may sometimes match the observed motion very poorly, although the estimates of the fundamental frequency are very close to those obtained using higher order models. Two-mode models usually can be fit to the output with very good results, while three-mode models are very difficult to treat, due to the large numbers of parameters involved. Figures 5.2a and 5.2b show the graphic output of the estimation program (MUMOID) (see DiPasquale and Cakmak, 1987) for the structure FW4, run 2, time window between 1 sec and 2 sec. Four plots are provided in the standard graphic output of MUMOID: basement (input) motion, observed upper level motion (continuous line) and predicted upper level motion (dotted line), prediction error and autocorrelation function of the prediction error. In Figure 5.2a, only one mode is used to fit the data, resulting in a poor match. In Figure 5.2b a two mode model is used with an apparent improvement.

In the computation of the maximum softening there are two sources of error. The first source of error is the uncertainties involved in the computation of $(T_0)_{max}$. When the structure is in the nonlinear regime, the equivalent linear parameters vary with time. The values estimated depend upon the particular time window selected. In addition, some statistical errors would be present even in the case of purely linear structures. When the structure is in the linear regime it is possible to obtain approximate expressions for the covariance matrix of the parameter estimates (DiPasquale and Cakmak, 1987). When nonlinearities are present, these same expressions will give information on the accuracy of the estimates computed.

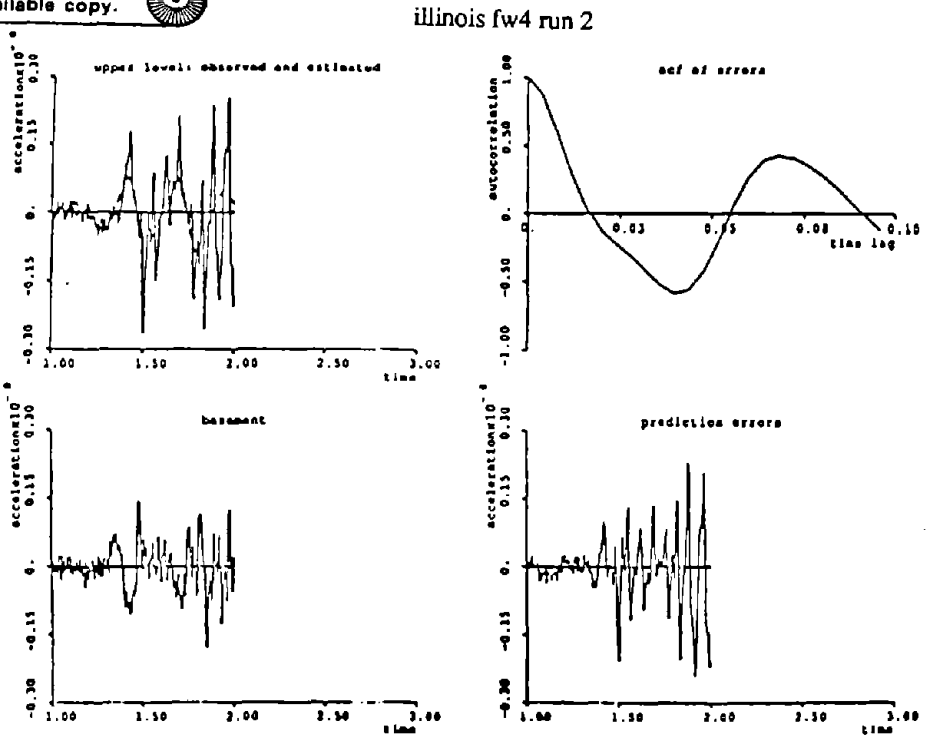

Figure 5.2a: Example of Analysis using a One-Mode Model

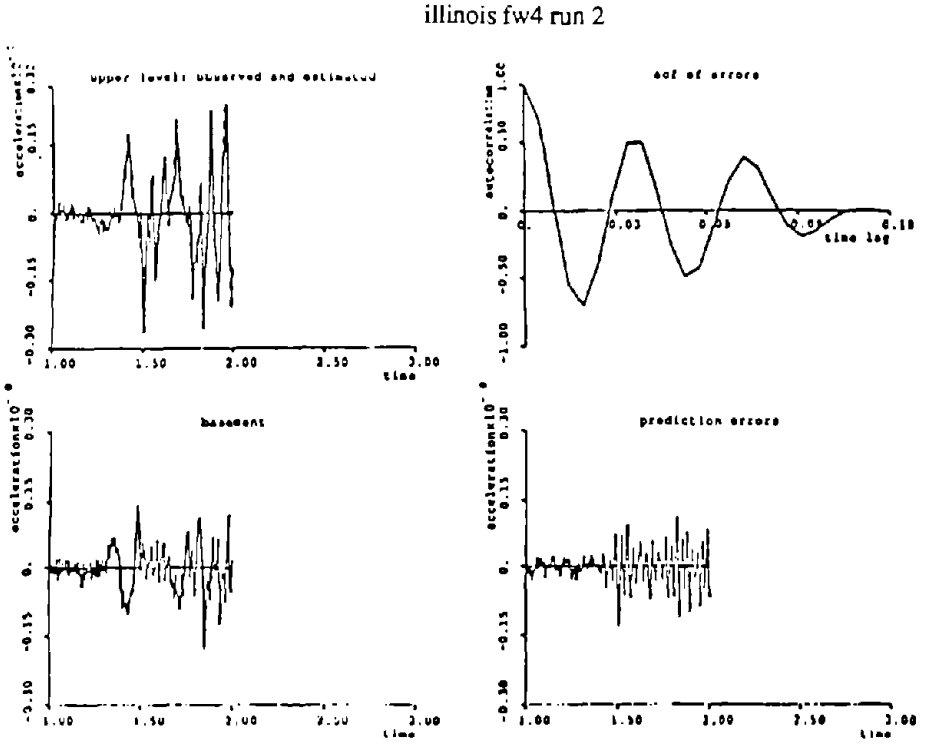

Figure 5.2b: Example of Analysis using a Two-Mode Model

The second source of error lies in the uncertainties in the values of $(T_0)_{initial}$ selected. In the analysis presented here, $(T_0)_{initial}$ has been estimated from the earthquake records relative to the first run, as would be the case if a real structure was analyzed and no prior information was available. In order to estimate $(T_0)_{initial}$, it is important that the structure's behavior is linear in the interval analyzed. Therefore, very short intervals close to the beginning of the record have been selected. For the structure H2, for which the first earthquake had a much smaller intensity than for the other structures, the "initial" time window was chosen so that the intensity of the input motion considered was the same as the intensity of the corresponding windows for the other structures.

5.4. Definition of Fragility Curves

A fragility curve gives the probability of exceedance for a given limit state as a function of a measurable structural parameter. From the analysis of the UIUC database, the authors (DiPasquale and Cakmak, 1988) have defined a fragility curve for the structural serviceability limit state. The probability of exceedance of the serviceability limit state is shown in Figure 5.3 as a function of the maximum softening. It represents the probability of the onset of structural damage, given the value of the maximum softening estimated from the strong motion records.

Further analysis of the UIUC database allows us to relate global damage indices (in particular, the maximum softening δ_M) with local quantities, namely the maximum interstory ductility developed during the strong motion. A set of fragility curves, relative to a sequence of limit states, can thus be defined.

Towards this goal, the maximum interstory ductility experienced by the structures during the earthquake simulation tests must first be evaluated. In the following, the ductility μ_i developed at the *ith* level will be defined as

$$\mu_i = \frac{\gamma_i}{\gamma_y} \tag{5.4.1}$$

where γ_i is the maximum story drift observed for the *ith* story and γ_y is the yielding drift of the story element, which in this case can be assumed to be equal for all stories.

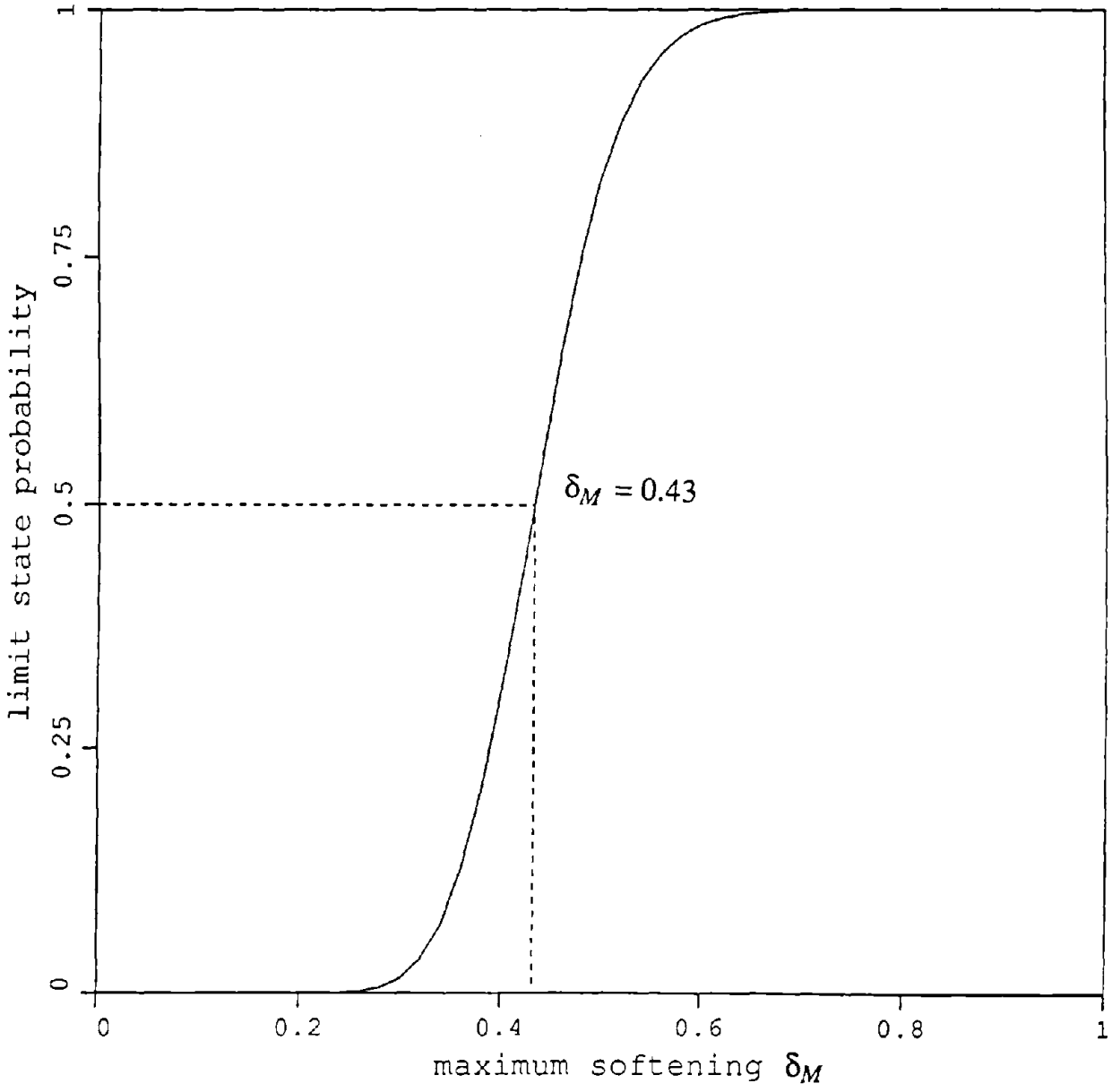

Figure 5.3: Fragility Curve, Structural Serviceability Limit State

The experimenters reports provide us with the maximum interstory drift observed during each run. The experimenters' reports also provide us (cfr. for instance Cecen, 1979) with an idealized trilinear characteristic for the story element considered, whence γ_y can be approximately evaluated. The value used in the following study is

$$\gamma_y = 0.5\% \tag{5.4.2}$$

Such a value for the yielding ductility is very sound from an engineering point of view, and is consistent with other authors' studies (e.g. Okamoto, 1984, or Sozen, 1981).

In the range of values observed in the UIUC database, the maximum interstory ductility μ and the maximum softening δ_M show an excellent correlation (Figure 5.4). The scatter of the data suggest that a linear model

$$\mu = \alpha + \beta\delta_M \tag{5.4.3}$$

can well describe the relationship between the maximum softening and the maximum ductility in the range $1 \leq \mu \leq 11$, which corresponds to light to critical structural damage. The values estimated for the parameters α and β of the regression are:
$\bar{\alpha} = -7.002$
$\bar{\beta} = 21.64$

with standard deviations:
$\sigma_\alpha = 1.181$
$\sigma_\beta = 1.986$
For simplicity the covariance $\sigma_{\alpha\beta}$ of the regression parameters has been neglected. α and β are therefore treated as independent random variables.

In order to define a set of fragility curves, an engineering definition of structural limit states must be used. All along in the field of structural damage prediction, the interstory ductility or the interstory drift have been associated to different degrees of damage. Sozen (1981) proposed that the maximum story drift be considered as the controlling parameter in the seismic damage of reinforced structures. The inherent randomness of the phenomenon led him to suggest an acceptability quotient A based on γ:

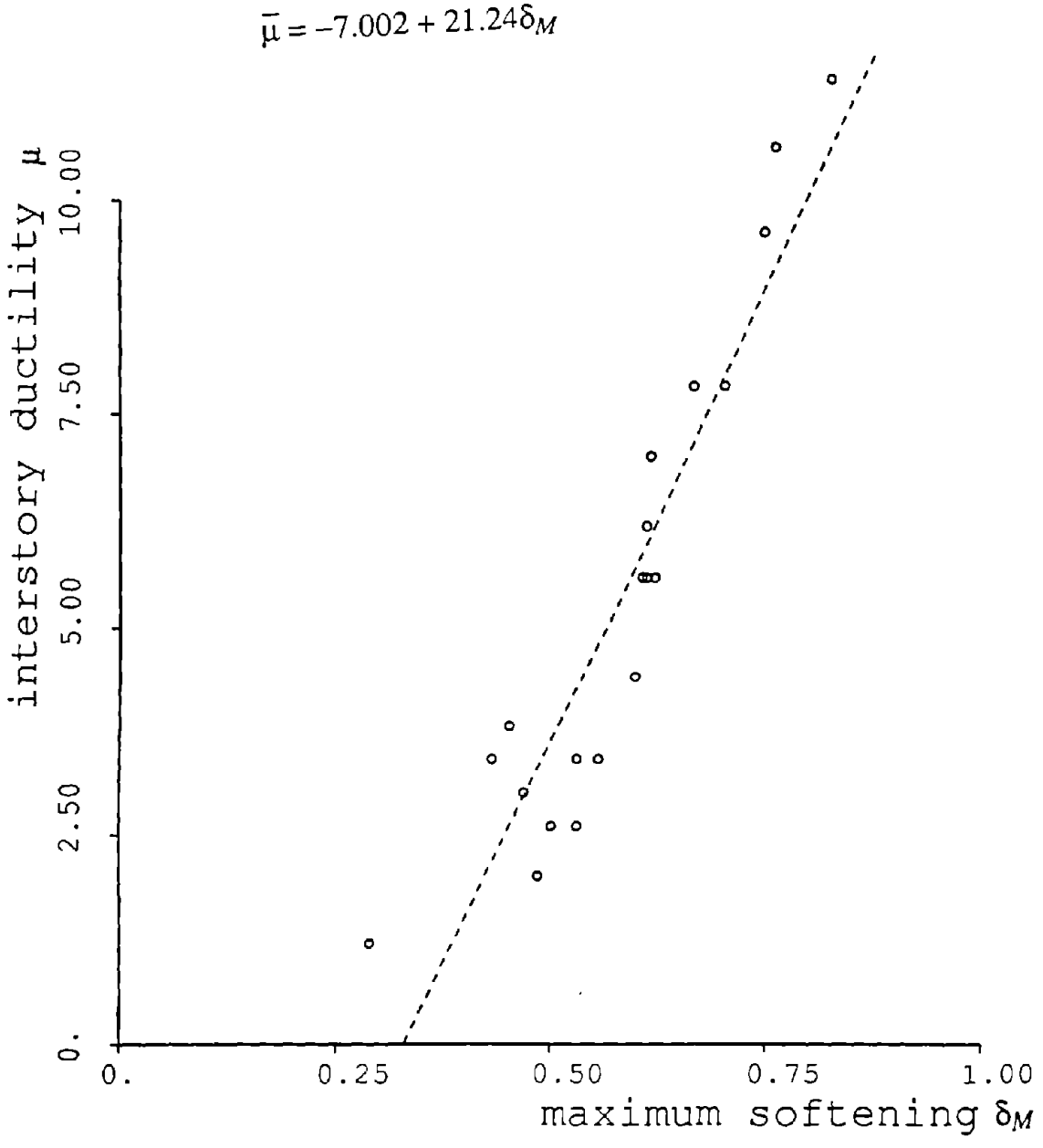

Figure 5.4: Interstory Ductility Ratio vs. Maximum Softening
for the UIUC Database
(dotted line: regression line)

$$A = \frac{(5 - 2\gamma)}{4} \qquad (5.4.4)$$

In the equation above, γ is the maximum story drift in percentage and A ($0 \leq A \leq 1$) represents the fraction of structures that are expected to remain safe after experiencing a story drift equal to γ. For example, a story drift of 0.5% will be always acceptable, whereas in as many as three-fourths of the cases a story drift of 2% will provoke damage.

Aktan and Bertero (1985) defined five limit states representing nonstructural damage, slight structural damage, moderate structural damage, severe structural damage and collapse as a function of the observed ductility ratio. Jaw and Hwang (1988) used this definition of limit states for a seismic reliability study of reinforced concrete structures using Montecarlo simulation. The value of interstory ductility at which the limit state is exceeded is assumed to be a lognormally distributed random variable with median μ_R and coefficient of variation β_R. The median value μ_R and the coefficient of variation β_R corresponding to each limit state are indicated in Table 5-3.

In this study, it is assumed that the values of Table 5-3, in principle valid only for shear wall structures, can be extended to the analysis of a general reinforced concrete structure. Further, in this preliminary phase of the research, the limit state is assumed to be determined by a value of the maximum interstory ductility μ_R equal to $\bar{\mu}_R$, i.e. the coefficient of variation relative to a limit state is assumed to be negligible.

For the purpose of damage detection, the maximum softening $\bar{\delta}_M$ is estimated from the analysis of strong motion records. An expected value $\bar{\mu}$ for the normalized intensity is easily computed:

$$\bar{\mu} = \bar{\alpha} + \bar{\beta}\, \delta_M \qquad (5.4.5)$$

The uncertainties present in the problem can be easily taken into account if it is assumed that α and β are independent random variables with means $\bar{\alpha}$ and $\bar{\beta}$ and standard deviation σ_α and σ_β. The variance of the maximum interstory ductility will then be:

Table 5-3: Ductility Capacity		
Limit State	$\bar{\mu}_R$	β_R
(1) Nonstructural Damage	1.0	0.3
(2) Slight Structural Damage	2.0	0.3
(3) Moderate Structural Damage	4.0	0.3
(4) Severe Structural Damage	6.0	0.3
(5) Collapse	7.5	0.3

$$\sigma_{\mu}^2 = \sigma_{\alpha}^2 + \delta_M^2 \sigma_{\beta}^2 \qquad (5.4.6)$$

In this model, the maximum interstory ductility μ is a gaussian random variable. It is possible to compute the probability that the interstory ductility μ_R, relative to any of the limit states of Table 5-3, has been exceeded:

$$P\ [\ \mu > \mu_R\ |\ \bar{\mu}] = erf\ (\frac{\mu_R - \bar{\mu}}{\sigma_{\mu}}) \qquad (5.4.7)$$

For each of the limit states considered, it is now possible to draw a fragility curve, which gives the probability of exceedance of the limit state considered as a function of the maximum softening estimated from strong motion records (Figure 5.5). It should be pointed out that the fragility curve, relative to the limit state of light structural damage (μ_R=2) practically coincides with the structural serviceability fragility curve of Figure 5.3.

5.5. Application to Simulated Earthquake Response

The model described above enables the investigator to predict the maximum interstory drift, which is a local quantity that cannot, in general, be measured, from the maximum softening, which can instead be estimated from earthquake records. The expected value $\bar{\gamma}$ of the interstory drift γ, defined as the ratio between the maximum interstory displacement and the story height, would be given by:

$$\bar{\gamma} = -0.0351 + 0.1082\delta_M \qquad (5.5.1)$$

The simulated response of a nonlinear multi-degree of freedom structure, modelling a typical reinforced concrete Japanese building was studied by Miyamura et. al. (1989), within the joint research project between Princeton University and Kajima Corp., Japan. The building considered was a reinforced concrete, 12-story structure . The resistance to lateral loads was provided by five 3-bay frames acting in parallel. The structure was modeled as an equivalent bend-shear beam, considering the nonlinear characteristics of each frame. A trilinear model was chosen for the force-deformation curves for a story element in each frame. The structure thus modeled is then subjected

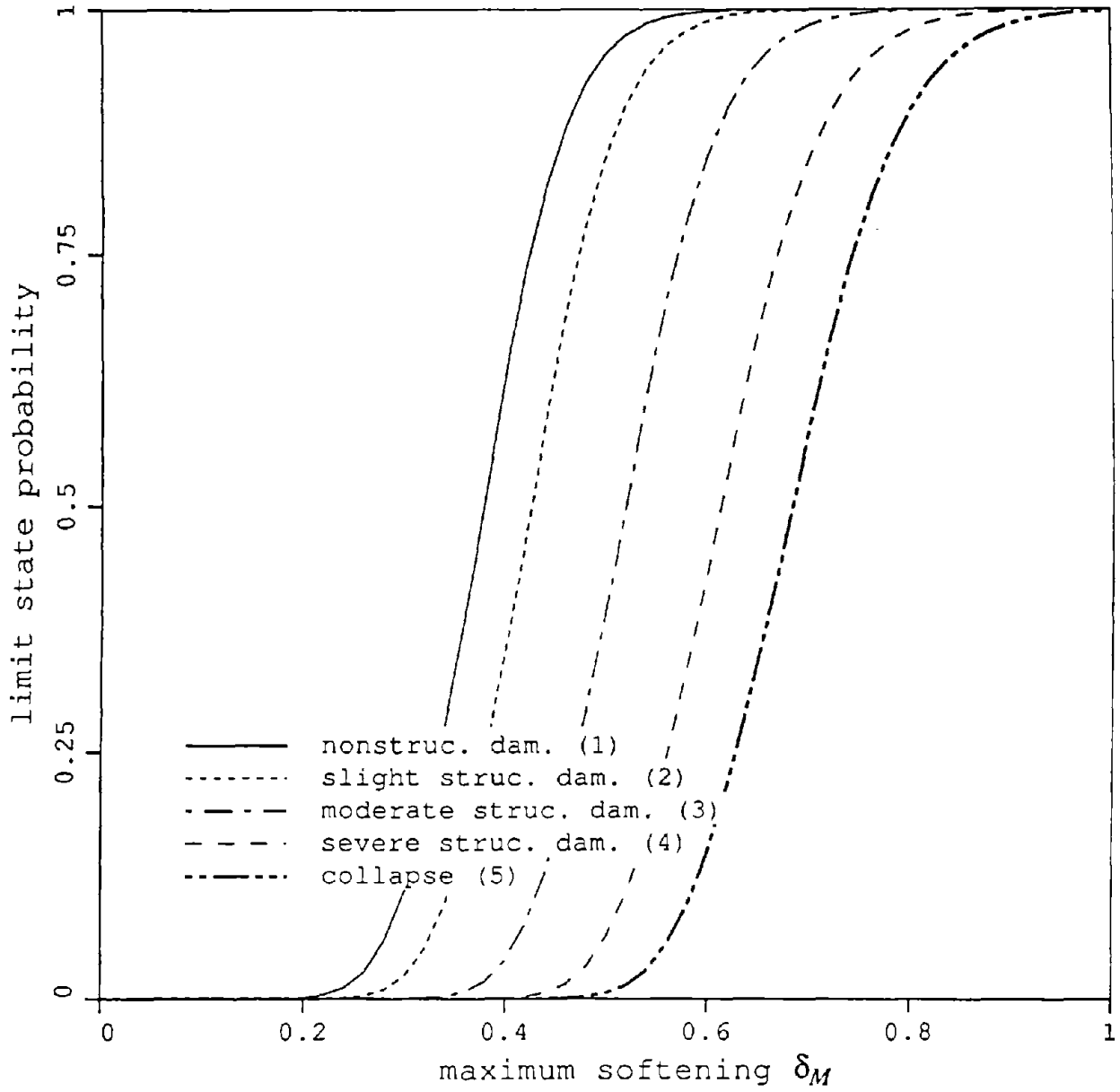

Figure 5.5: Fragility Curves for Five Structural Limit States

to earthquake-like excitation. For this numerical experiments, the recorded motion at the Tarumizu Dam, during the Miyagiken-Oki earthquake (1978) was selected as input motion. In order to simulate structural response to earthquakes of different intensity, the recorded motion was multiplied by a constant amplification factor. Ten different waveforms, ranging from peak acceleration $a_{max} = 0.18g$ (corresponding to the original earthquake wave) to $a_{max} = 1.81g$ (for which the original wave had been amplified 10 times) were then obtained. The maximum softening, as well as the maximum interstory drift, were then obtained from the simulated earthquake response.

Figure 5.6 shows the actual maximum interstory drift vs. the predicted, using equation (5.5.1). As it can be seen, the agreement is very good. Figure 5.7 shows the fragility analysis for the building in question. The model developed in this report enables us to give an assessment of the structural damage for each simulated earthquake. In particular, we can that the structure experiences almost no damage for $a_{max}<0.8g$, while slight to moderate damage occurs for higher intensity of the earthquake ground motion, as it could be expected, given the very conservative design that is used in Japan.

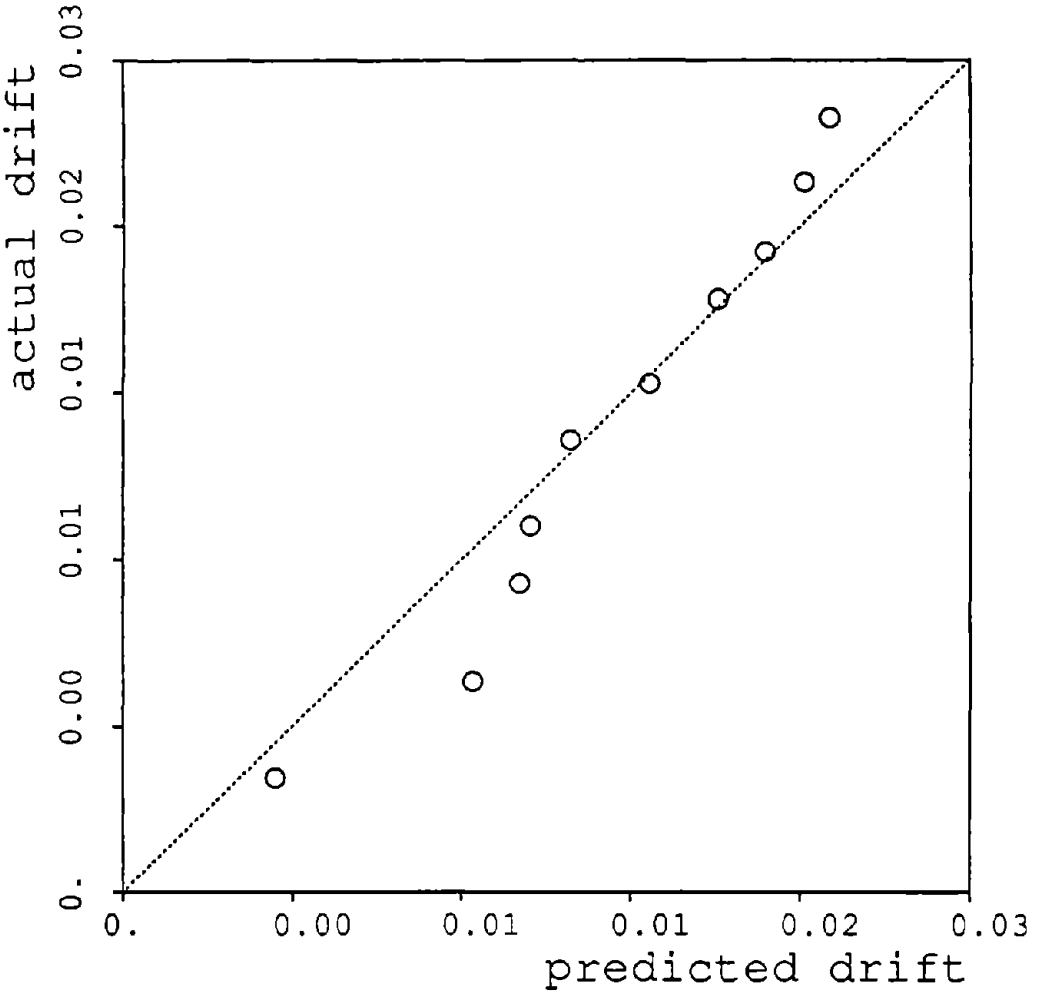

Figure 5.6: Comparison between Actual and Predicted Maximum Story Drift

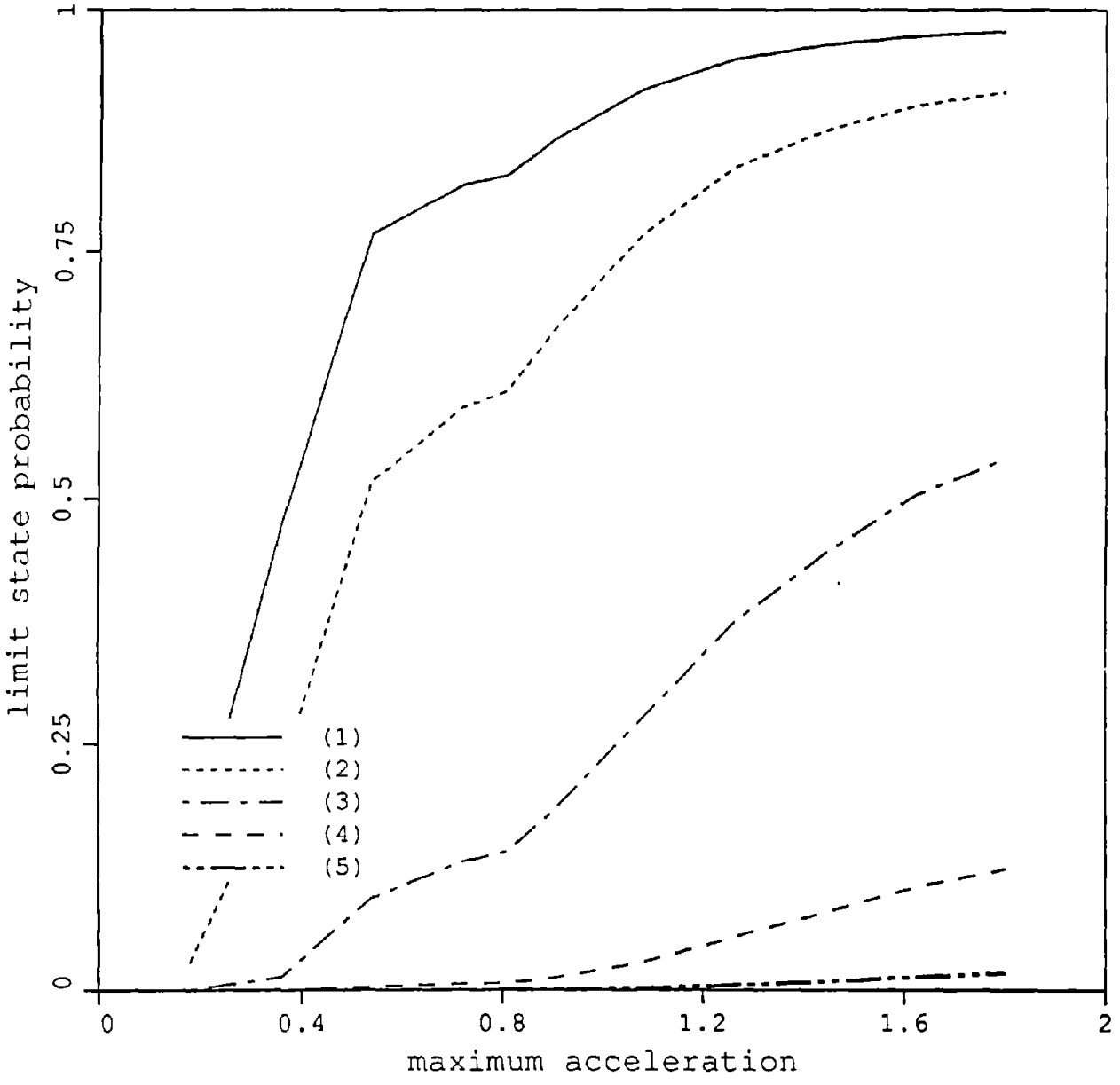

Figure 5.7: Fragility Analysis for a Simulated
12-Story, Reinforced Concrete Building

SECTION 6: CONCLUSIONS

For the cases of elastic and of elasto-plastic damage, a relationship between parameter-based global damage indices and local damage variables has been established. This gives a theoretical (thermodynamic) foundation to such global damage indices, and opens new areas of research. For the case of damage in reinforced concrete structures, stiffness degradation can be related to microcracking of concrete, and plastic deformation related to yielding of reinforcement bars. The identification of such independent contributions, which can both be related to local phenomena, will foster new and more effective models for damage analysis.

The results presented in this report, regarding the relationship between parameter-based global damage indices (the final softening δ_f) and local stiffness degradation, can be also used in the analysis of aging structures. The degradation of the low-amplitude characteristic of existing structures can in fact be quantified by monitoring the frequencies of vibration.

The relationship established between parameter-based global damage indices (in particular the plastic softening δ_p) and the plastic deformation that is experienced by the material at the local level can be of immediate use for damage assessment. Many authors (see for example Chung et al., 1988) relate plastic deformation of reinforced concrete elements to the degradation of the element's strength. If an average measure of the residual strength of a structure is obtained it will be possible to assess the resistance of the structure to future load events.

Under the assumption of independence of the contributions of stiffness degradation and of plastic deformation to the global damage state of a structure, only one damage index, the maximum softening δ_M, is necessary to define the global damage state of a structure. Hence, fragility curves, providing the probability of exceedance of structural limit states as a function of δ_M, have been obtained. These curve can provide a practical tool for post-earthquake damage assessment of instrumented buildings.

SECTION 7: REFERENCES

(1) Abrams, D.P., and Sozen, M.T., (1979), "Experimental Study of Frame-Wall Interaction in Reinforced Concrete Structures Subjected to Strong Earthquake Motions", Report No. SRS 460, UILU-ENG-79-2002, University of Illinois at Urbana-Champaign.

(2) Aktan, A.E., Bertero, V.V., "R.C. Structural Walls: Seismic Design for Shear", *ASCE J. Struc. Eng.*, Vol. 111, No. 8, August 1985, pp. 1775-1791.

(3) Beck, J.L., (1979), "Determining Models of Structure from Earthquake Records", Ph.D. Dissertation, California Institute of Technology, 1978.

(4) Cecen, H., (1979), "Response of Ten Story, Reinforced Concrete Models Frames to Simulated Earthquakes", Ph.D. Dissertation, University of Illinois at Urbana-Champaign, 1979.

(5) Chung, Y.S., Meyer, C., and Shinozuka, M. (1987), "Seismic Damage Assessment of Reinforced Concrete Members", Technical Report NCEER-87-0022, National Center for Earhquake Engineering Research, State University of New York at Buffalo, October 1987.

(6) DiPasquale, E., and Çakmak, A.S., (1987) "Detection and Assessment of Seismic Structural Damage", Report NCCER-87-0015, National Center for Earthquake Engineering Research, State University of New York at Buffalo, August 1987.

(7) DiPasquale, E., and Çakmak, A.S., (1988) "Identification of the Serviceability Limit State and Detection of Seismic Structural Damage", Report NCCER-88-0022, National Center for Earthquake Engineering Research, State University of New York at Buffalo, June 1988.

(8) Dowell,E.H., (1979), "On Some General Properties of Combined Dynamical Systems", *ASME J. App. Mech.*, Vol.46, March 1979, pp. 206-209.

(9) Healey,T.J., and Sozen,M.A., (1978), "Experimental Study of the Dynamic Response of a Ten Story Reinforced Concrete Frame with a Tall First Story", Rep. No. UILU-ENG-78-2012, SRS 450, University of Illinois, Urbana, Ill..

(10) Jaw, J.-W., Hwang, H. H.-M., "Seismic Fragility Analysis of Shear Wall Structures", Technical Report NCEER-88-0009, National Center for Earhquake Engineering Research, State University of New York at Buffalo, April 1988.

(11) Ju, J. W., (1988), "On Energy-Based Coupled Elasto-Plastic Damage Theories: Constitutive Modeling and Computational Aspects", *Intl. J. of Solids and Struc.*, accepted for publication.

(12) Ju, J. W., Monteiro, P.J.M., and Rashed, A.I. (1989), "On Continuum Damage of Cement Paste and Mortar as Affected by Porosity and Sand Concentration", *ASCE J. Eng. Mech.*, Vol. 115, No. 1, pp. 105-130.

(13) Kachanov, L. M. (1958), "Time of the Rupture Process under Creep Conditions", IVZ AKAD Nauk, *S.S.R., Otd Tech Nauk* No. 8, pp. 26-31.

(14) Kachanov, L. M. (1986), Introduction to Continuum Damage Mechanics, Dordrecht ; Boston : M. Nijhoff.

(15) Krajcinovic, D., (1984), "Continuum Damage Mechanics", *Appl. Mech. Review.* Vol. 37: 1-6, pp. 397-402.

(16) Krajcinovic, D., and Fonseca, G. U. (1981), "The Continuous Damage Theory of Brittle Materials", Parts I and II, *ASME J. App. Mech.* 48, pp. 809-824.

(17) Lemaitre, J., (1984), "How to Use Damage Mechanics", *Nuc. Eng. Des.*, 80, pp. 233-245.

(18) M. Miyamura, K. Kanda, K. Kato, E. DiPasquale, S. Rodriguez-Gomez and A.S. Cakmak, "Global Damage Indices and Nonlinear Structural Response", to be presented at the 5th ICOSSAR, San Francisco, Ca, August 1989.

(19) Okamoto, S. (1984), "Introduction to Earthquake Engineering", University of Tokyo Press, 1984.

(20) Park,Y.-J.,Ang, A. H.-S., and Wen, Y. K., (1985), "Seismic Damage Analysis of Reinforced Concrete Buildings", *ASCE J. Struc. Eng.*, 111 (4) April 1985, pp. 740-757.

(21) Rayleigh, J.(1894), "The Theory of Sound", Dover Publ..

(22) Simo, J. C., and Ju, J.W. (1987a), "Strain- and Stress-Based Continuum Damage Models - I. Formulation", *Int. J. Solids Struc.*, Vol. 23, No. 7, pp. 821-840.

(23) Simo, J. C., and Ju, J.W. (1987b), "Strain- and Stress-Based Continuum Damage Models - II. Applications", *Int. J. Solids Struc.*, Vol. 23, No. 7, pp. 841-869.

(24) Sozen, M.A., (1981), "Review of Earthquake Response of Reinforced Concrete Buildings with a View to Drift Control", State of the Art in Earthquake Engineering, Turkish National Committee on Earthquake Engineering,

Istanbul,Turkey 1981.

(25) Stephens, J.E., and Yao, J.P.T., (1987), "Damage Assessment Using Response Measurements", *ASCE J. Struc. Eng.* 113 (4) April 1987, pp. 787-801

(26) Toussi, S., and Yao, J.P.T., (1983), "Assessment of Structural Damage Using the Theory of Evidence", *Structural Safety,* 1 (1982/1983), pp. 107-121.

(27) Yao,J.P.T., (1982) "Probabilistic Method for the Evaluation of Seismic Damage of Existing Structures", *Soil Dyn. Earth. Eng.*, Vol. 1, No. 3, 1982, pp. 130-135.

NATIONAL CENTER FOR EARTHQUAKE ENGINEERING RESEARCH
LIST OF PUBLISHED TECHNICAL REPORTS

The National Center for Earthquake Engineering Research (NCEER) publishes technical reports on a variety of subjects related to earthquake engineering written by authors funded through NCEER. These reports are available from both NCEER's Publications Department and the National Technical Information Service (NTIS). Requests for reports should be directed to the Publications Department, National Center for Earthquake Engineering Research, State University of New York at Buffalo, Red Jacket Quadrangle, Buffalo, New York 14261. Reports can also be requested through NTIS, 5285 Port Royal Road, Springfield, Virginia 22161. NTIS accession numbers are shown in parenthesis, if available.

NCEER-87-0001 "First-Year Program in Research, Education and Technology Transfer," 3/5/87, (PB88-134275/AS).

NCEER-87-0002 "Experimental Evaluation of Instantaneous Optimal Algorithms for Structural Control," by R.C. Lin, T.T. Soong and A.M. Reinhorn, 4/20/87, (PB88-134341/AS).

NCEER-87-0003 "Experimentation Using the Earthquake Simulation Facilities at University at Buffalo," by A.M. Reinhorn and R.L. Ketter, to be published.

NCEER-87-0004 "The System Characteristics and Performance of a Shaking Table," by J.S. Hwang, K.C. Chang and G.C. Lee, 6/1/87, (PB88-134259/AS). This report is available only through NTIS (see address given above).

NCEER-87-0005 "A Finite Element Formulation for Nonlinear Viscoplastic Material Using a Q Model," by O. Gyebi and G. Dasgupta, 11/2/87, (PB88-213764/AS).

NCEER-87-0006 "Symbolic Manipulation Program (SMP) - Algebraic Codes for Two and Three Dimensional Finite Element Formulations," by X. Lee and G. Dasgupta, 11/9/87, (PB88-219522/AS).

NCEER-87-0007 "Instantaneous Optimal Control Laws for Tall Buildings Under Seismic Excitations," by J.N. Yang, A. Akbarpour and P. Ghaemmaghami, 6/10/87, (PB88-134333/AS).

NCEER-87-0008 "IDARC: Inelastic Damage Analysis of Reinforced Concrete Frame - Shear-Wall Structures," by Y.J. Park, A.M. Reinhorn and S.K. Kunnath, 7/20/87, (PB88-134325/AS).

NCEER-87-0009 "Liquefaction Potential for New York State: A Preliminary Report on Sites in Manhattan and Buffalo," by M. Budhu, V. Vijayakumar, R.F. Giese and L. Baumgras, 8/31/87, (PB88-163704/AS). This report is available only through NTIS (see address given above).

NCEER-87-0010 "Vertical and Torsional Vibration of Foundations in Inhomogeneous Media," by A.S. Veletsos and K.W. Dotson, 6/1/87, (PB88-134291/AS).

NCEER-87-0011 "Seismic Probabilistic Risk Assessment and Seismic Margins Studies for Nuclear Power Plants," by Howard H.M. Hwang, 6/15/87, (PB88-134267/AS). This report is available only through NTIS (see address given above).

NCEER-87-0012 "Parametric Studies of Frequency Response of Secondary Systems Under Ground-Acceleration Excitations," by Y. Yong and Y.K. Lin, 6/10/87, (PB88-134309/AS).

NCEER-87-0013 "Frequency Response of Secondary Systems Under Seismic Excitation," by J.A. HoLung, J. Cai and Y.K. Lin, 7/31/87, (PB88-134317/AS).

NCEER-87-0014 "Modelling Earthquake Ground Motions in Seismically Active Regions Using Parametric Time Series Methods," by G.W. Ellis and A.S. Cakmak, 8/25/87, (PB88-134283/AS).

NCEER-87-0015 "Detection and Assessment of Seismic Structural Damage," by E. DiPasquale and A.S. Cakmak, 8/25/87, (PB88-163712/AS).

NCEER-87-0016 "Pipeline Experiment at Parkfield, California," by J. Isenberg and E. Richardson, 9/15/87, (PB88-163720/AS).

NCEER-87-0017 "Digital Simulation of Seismic Ground Motion," by M. Shinozuka, G. Deodatis and T. Harada, 8/31/87, (PB88-155197/AS). This report is available only through NTIS (see address given above).

NCEER-87-0018 "Practical Considerations for Structural Control: System Uncertainty, System Time Delay and Truncation of Small Control Forces," J.N. Yang and A. Akbarpour, 8/10/87, (PB88-163738/AS).

NCEER-87-0019 "Modal Analysis of Nonclassically Damped Structural Systems Using Canonical Transformation," by J.N. Yang, S. Sarkani and F.X. Long, 9/27/87, (PB88-187851/AS).

NCEER-87-0020 "A Nonstationary Solution in Random Vibration Theory," by J.R. Red-Horse and P.D. Spanos, 11/3/87, (PB88-163746/AS).

NCEER-87-0021 "Horizontal Impedances for Radially Inhomogeneous Viscoelastic Soil Layers," by A.S. Veletsos and K.W. Dotson, 10/15/87, (PB88-150859/AS).

NCEER-87-0022 "Seismic Damage Assessment of Reinforced Concrete Members," by Y.S. Chung, C. Meyer and M. Shinozuka, 10/9/87, (PB88-150867/AS). This report is available only through NTIS (see address given above).

NCEER-87-0023 "Active Structural Control in Civil Engineering," by T.T. Soong, 11/11/87, (PB88-187778/AS).

NCEER-87-0024 Vertical and Torsional Impedances for Radially Inhomogeneous Viscoelastic Soil Layers," by K.W. Dotson and A.S. Veletsos, 12/87, (PB88-187786/AS).

NCEER-87-0025 "Proceedings from the Symposium on Seismic Hazards, Ground Motions, Soil-Liquefaction and Engineering Practice in Eastern North America," October 20-22, 1987, edited by K.H. Jacob, 12/87, (PB88-188115/AS).

NCEER-87-0026 "Report on the Whittier-Narrows, California, Earthquake of October 1, 1987," by J. Pantelic and A. Reinhorn, 11/87, (PB88-187752/AS). This report is available only through NTIS (see address given above).

NCEER-87-0027 "Design of a Modular Program for Transient Nonlinear Analysis of Large 3-D Building Structures," by S. Srivastav and J.F. Abel, 12/30/87, (PB88-187950/AS).

NCEER-87-0028 "Second-Year Program in Research, Education and Technology Transfer," 3/8/88, (PB88-219480/AS).

NCEER-88-0001 "Workshop on Seismic Computer Analysis and Design of Buildings With Interactive Graphics," by W. McGuire, J.F. Abel and C.H. Conley, 1/18/88, (PB88-187760/AS).

NCEER-88-0002 "Optimal Control of Nonlinear Flexible Structures," by J.N. Yang, F.X. Long and D. Wong, 1/22/88, (PB88-213772/AS).

NCEER-88-0003 "Substructuring Techniques in the Time Domain for Primary-Secondary Structural Systems," by G.D. Manolis and G. Juhn, 2/10/88, (PB88-213780/AS).

NCEER-88-0004 "Iterative Seismic Analysis of Primary-Secondary Systems," by A. Singhal, L.D. Lutes and P.D. Spanos, 2/23/88, (PB88-213798/AS).

NCEER-88-0005 "Stochastic Finite Element Expansion for Random Media," by P.D. Spanos and R. Ghanem, 3/14/88, (PB88-213806/AS).

NCEER-88-0006 "Combining Structural Optimization and Structural Control," by F.Y. Cheng and C.P. Pantelides, 1/10/88, (PB88-213814/AS).

NCEER-88-0007 "Seismic Performance Assessment of Code-Designed Structures," by H.H-M. Hwang, J-W. Jaw and H-J. Shau, 3/20/88, (PB88-219423/AS).

NCEER-88-0008 "Reliability Analysis of Code-Designed Structures Under Natural Hazards," by H.H-M. Hwang, H. Ushiba and M. Shinozuka, 2/29/88, (PB88-229471/AS).

NCEER-88-0009 "Seismic Fragility Analysis of Shear Wall Structures," by J-W Jaw and H.H-M. Hwang, 4/30/88, (PB89-102867/AS).

NCEER-88-0010 "Base Isolation of a Multi-Story Building Under a Harmonic Ground Motion - A Comparison of Performances of Various Systems," by F-G Fan, G. Ahmadi and I.G. Tadjbakhsh, 5/18/88, (PB89-122238/AS).

NCEER-88-0011 "Seismic Floor Response Spectra for a Combined System by Green's Functions," by F.M. Lavelle, L.A. Bergman and P.D. Spanos, 5/1/88, (PB89-102875/AS).

NCEER-88-0012 "A New Solution Technique for Randomly Excited Hysteretic Structures," by G.Q. Cai and Y.K. Lin, 5/16/88, (PB89-102883/AS).

NCEER-88-0013 "A Study of Radiation Damping and Soil-Structure Interaction Effects in the Centrifuge," by K. Weissman, supervised by J.H. Prevost, 5/24/88, (PB89-144703/AS).

NCEER-88-0014 "Parameter Identification and Implementation of a Kinematic Plasticity Model for Frictional Soils," by J.H. Prevost and D.V. Griffiths, to be published.

NCEER-88-0015 "Two- and Three- Dimensional Dynamic Finite Element Analyses of the Long Valley Dam," by D.V. Griffiths and J.H. Prevost, 6/17/88, (PB89-144711/AS).

NCEER-88-0016 "Damage Assessment of Reinforced Concrete Structures in Eastern United States," by A.M. Reinhorn, M.J. Seidel, S.K. Kunnath and Y.J. Park, 6/15/88, (PB89-122220/AS).

NCEER-88-0017 "Dynamic Compliance of Vertically Loaded Strip Foundations in Multilayered Viscoelastic Soils," by S. Ahmad and A.S.M. Israil, 6/17/88, (PB89-102891/AS).

NCEER-88-0018 "An Experimental Study of Seismic Structural Response With Added Viscoelastic Dampers," by R.C. Lin, Z. Liang, T.T. Soong and R.H. Zhang, 6/30/88, (PB89-122212/AS).

NCEER-88-0019 "Experimental Investigation of Primary - Secondary System Interaction," by G.D. Manolis, G. Juhn and A.M. Reinhorn, 5/27/88, (PB89-122204/AS).

NCEER-88-0020 "A Response Spectrum Approach For Analysis of Nonclassically Damped Structures," by J.N. Yang, S. Sarkani and F.X. Long, 4/22/88, (PB89-102909/AS).

NCEER-88-0021 "Seismic Interaction of Structures and Soils: Stochastic Approach," by A.S. Veletsos and A.M. Prasad, 7/21/88, (PB89-122196/AS).

NCEER-88-0022 "Identification of the Serviceability Limit State and Detection of Seismic Structural Damage," by E. DiPasquale and A.S. Cakmak, 6/15/88, (PB89-122188/AS).

NCEER-88-0023 "Multi-Hazard Risk Analysis: Case of a Simple Offshore Structure," by B.K. Bhartia and E.H. Vanmarcke, 7/21/88, (PB89-145213/AS).

NCEER-88-0024 "Automated Seismic Design of Reinforced Concrete Buildings," by Y.S. Chung, C. Meyer and M. Shinozuka, 7/5/88, (PB89-122170/AS).

NCEER-88-0025 "Experimental Study of Active Control of MDOF Structures Under Seismic Excitations," by L.L. Chung, R.C. Lin, T.T. Soong and A.M. Reinhorn, 7/10/88, (PB89-122600/AS).

NCEER-88-0026 "Earthquake Simulation Tests of a Low-Rise Metal Structure," by J.S. Hwang, K.C. Chang, G.C. Lee and R.L. Ketter, 8/1/88, (PB89-102917/AS).

NCEER-88-0027 "Systems Study of Urban Response and Reconstruction Due to Catastrophic Earthquakes," by F. Kozin and H.K. Zhou, 9/22/88.

NCEER-88-0028 "Seismic Fragility Analysis of Plane Frame Structures," by H.H-M. Hwang and Y.K. Low, 7/31/88, (PB89-131445/AS).

NCEER-88-0029 "Response Analysis of Stochastic Structures," by A. Kardara, C. Bucher and M. Shinozuka, 9/22/88, (PB89-174429/AS).

NCEER-88-0030 "Nonnormal Accelerations Due to Yielding in a Primary Structure," by D.C.K. Chen and L.D. Lutes, 9/19/88, (PB89-131437/AS).

NCEER-88-0031 "Design Approaches for Soil-Structure Interaction," by A.S. Veletsos, A.M. Prasad and Y. Tang, 12/30/88, (PB89-174437/AS).

NCEER-88-0032 "A Re-evaluation of Design Spectra for Seismic Damage Control," by C.J. Turkstra and A.G. Tallin, 11/7/88, (PB89-145221/AS).

NCEER-88-0033 "The Behavior and Design of Noncontact Lap Splices Subjected to Repeated Inelastic Tensile Loading," by V.E. Sagan, P. Gergely and R.N. White, 12/8/88, (PB89-163737/AS).

NCEER-88-0034 "Seismic Response of Pile Foundations," by S.M. Mamoon, P.K. Banerjee and S. Ahmad, 11/1/88, (PB89-145239/AS).

NCEER-88-0035 "Modeling of R/C Building Structures With Flexible Floor Diaphragms (IDARC2)," by A.M. Reinhorn, S.K. Kunnath and N. Panahshahi, 9/7/88, (PB89-207153/AS).

NCEER-88-0036 "Solution of the Dam-Reservoir Interaction Problem Using a Combination of FEM, BEM with Particular Integrals, Modal Analysis, and Substructuring," by C-S. Tsai, G.C. Lee and R.L. Ketter, 12/31/88, (PB89-207146/AS).

NCEER-88-0037 "Optimal Placement of Actuators for Structural Control," by F.Y. Cheng and C.P. Pantelides, 8/15/88, (PB89-162846/AS).

NCEER-88-0038 "Teflon Bearings in Aseismic Base Isolation: Experimental Studies and Mathematical Modeling," by A. Mokha, M.C. Constantinou and A.M. Reinhorn, 12/5/88, (PB89-218457/AS).

NCEER-88-0039 "Seismic Behavior of Flat Slab High-Rise Buildings in the New York City Area," by P. Weidlinger and M. Ettouney, 10/15/88.

NCEER-88-0040 "Evaluation of the Earthquake Resistance of Existing Buildings in New York City," by P. Weidlinger and M. Ettouney, 10/15/88, to be published.

NCEER-88-0041 "Small-Scale Modeling Techniques for Reinforced Concrete Structures Subjected to Seismic Loads," by W. Kim, A. El-Attar and R.N. White, 11/22/88, (PB89-189625/AS).

NCEER-88-0042 "Modeling Strong Ground Motion from Multiple Event Earthquakes," by G.W. Ellis and A.S. Cakmak, 10/15/88, (PB89-174445/AS).

NCEER-88-0043 "Nonstationary Models of Seismic Ground Acceleration," by M. Grigoriu, S.E. Ruiz and E. Rosenblueth, 7/15/88, (PB89-189617/AS).

NCEER-88-0044 "SARCF User's Guide: Seismic Analysis of Reinforced Concrete Frames," by Y.S. Chung, C. Meyer and M. Shinozuka, 11/9/88, (PB89-174452/AS).

NCEER-88-0045 "First Expert Panel Meeting on Disaster Research and Planning," edited by J. Pantelic and J. Stoyle, 9/15/88, (PB89-174460/AS).

NCEER-88-0046 "Preliminary Studies of the Effect of Degrading Infill Walls on the Nonlinear Seismic Response of Steel Frames," by C.Z. Chrysostomou, P. Gergely and J.F. Abel, 12/19/88, (PB89-208383/AS).

NCEER-88-0047 "Reinforced Concrete Frame Component Testing Facility - Design, Construction, Instrumentation and Operation," by S.P. Pessiki, C. Conley, T. Bond, P. Gergely and R.N. White, 12/16/88, (PB89-174478/AS).

NCEER-89-0001 "Effects of Protective Cushion and Soil Compliancy on the Response of Equipment Within a Seismically Excited Building," by J.A. HoLung, 2/16/89, (PB89-207179/AS).

NCEER-89-0002 "Statistical Evaluation of Response Modification Factors for Reinforced Concrete Structures," by H.H-M. Hwang and J-W. Jaw, 2/17/89, (PB89-207187/AS).

NCEER-89-0003 "Hysteretic Columns Under Random Excitation," by G-Q. Cai and Y.K. Lin, 1/9/89, (PB89-196513/AS).

NCEER-89-0004 "Experimental Study of 'Elephant Foot Bulge' Instability of Thin-Walled Metal Tanks," by Z-H. Jia and R.L. Ketter, 2/22/89, (PB89-207195/AS).

NCEER-89-0005 "Experiment on Performance of Buried Pipelines Across San Andreas Fault," by J. Isenberg, E. Richardson and T.D. O'Rourke, 3/10/89, (PB89-218440/AS).

NCEER-89-0006 "A Knowledge-Based Approach to Structural Design of Earthquake-Resistant Buildings," by M. Subramani, P. Gergely, C.H. Conley, J.F. Abel and A.H. Zaghw, 1/15/89, (PB89-218465/AS).

NCEER-89-0007 "Liquefaction Hazards and Their Effects on Buried Pipelines," by T.D. O'Rourke and P.A. Lane, 2/1/89, (PB89-218481).

NCEER-89-0008 "Fundamentals of System Identification in Structural Dynamics," by H. Imai, C-B. Yun, O. Maruyama and M. Shinozuka, 1/26/89, (PB89-207211/AS).

NCEER-89-0009 "Effects of the 1985 Michoacan Earthquake on Water Systems and Other Buried Lifelines in Mexico," by A.G. Ayala and M.J. O'Rourke, 3/8/89, (PB89-207229/AS).

NCEER-89-R010 "NCEER Bibliography of Earthquake Education Materials," by K.E.K. Ross, 3/10/89, (PB90-109901/AS).

NCEER-89-0011 "Inelastic Three-Dimensional Response Analysis of Reinforced Concrete Building Structures (IDARC-3D), Part I - Modeling," by S.K. Kunnath and A.M. Reinhorn, 4/17/89, (PB90-114612/AS).

NCEER-89-0012 "Recommended Modifications to ATC-14," by C.D. Poland and J.O. Malley, 4/12/89.

NCEER-89-0013 "Repair and Strengthening of Beam-to-Column Connections Subjected to Earthquake Loading," by M. Corazao and A.J. Durrani, 2/28/89, (PB90-109885/AS).

NCEER-89-0014 "Program EXKAL2 for Identification of Structural Dynamic Systems," by O. Maruyama, C-B. Yun, M. Hoshiya and M. Shinozuka, 5/19/89, (PB90-109877/AS).

NCEER-89-0015 "Response of Frames With Bolted Semi-Rigid Connections, Part I - Experimental Study and Analytical Predictions," by P.J. DiCorso, A.M. Reinhorn, J.R. Dickerson, J.B. Radziminski and W.L. Harper, 6/1/89, to be published.

NCEER-89-0016 "ARMA Monte Carlo Simulation in Probabilistic Structural Analysis," by P.D. Spanos and M.P. Mignolet, 7/10/89, (PB90-109893/AS).

NCEER-89-0017 "Preliminary Proceedings of the Conference on Disaster Preparedness - The Place of Earthquake Education in Our Schools, July 9-11, 1989," 6/23/89, (PB90-108606/AS).

NCEER-89-0018 "Multidimensional Models of Hysteretic Material Behavior for Vibration Analysis of Shape Memory Energy Absorbing Devices, by E.J. Graesser and F.A. Cozzarelli, 6/7/89.

NCEER-89-0019 "Nonlinear Dynamic Analysis of Three-Dimensional Base Isolated Structures (3D-BASIS)," by S. Nagarajaiah, A.M. Reinhorn and M.C. Constantinou, 8/3/89.

NCEER-89-0020 "Structural Control Considering Time-Rate of Control Forces and Control Rate Constraints," by F.Y. Cheng and C.P. Pantelides, 8/3/89.

NCEER-89-0021 "Subsurface Conditions of Memphis and Shelby County," by K.W. Ng, T-S. Chang and H-H.M. Hwang, 7/26/89.

NCEER-89-0022 "Seismic Wave Propagation Effects on Straight Jointed Buried Pipelines," by K. Elhmadi and M.J. O'Rourke, 8/24/89.

NCEER-89-0023 "Workshop on Serviceability Analysis of Water Delivery Systems," edited by M. Grigoriu, 3/6/89.

NCEER-89-0024 "Shaking Table Study of a 1/5 Scale Steel Frame Composed of Tapered Members," by K.C. Chang, J.S. Hwang and G.C. Lee, 9/18/89.

NCEER-89-0025 "DYNA1D: A Computer Program for Nonlinear Seismic Site Response Analysis - Technical Documentation," by Jean H. Prevost, 9/14/89.

NCEER-89-0026 "One-Quarter Scale Model Studies of Active Tendon Systems and Active Mass Dampers for Aseismic Protection," by A.M. Reinhorn, T.T. Soong, R.C. Lin, Y.P. Yang, Y. Fukao, H. Abe and M. Nakai, 9/15/89, to be published.

NCEER-89-0027 "Scattering of Waves by Inclusions in a Nonhomogeneous Elastic Half Space Solved by Boundary Element Methods," by P.K. Hadley, A. Askar and A.S. Cakmak, 6/15/89.

NCEER-89-0028 "Statistical Evaluation of Deflection Amplification Factors for Reinforced Concrete Structures," by H.H.M. Hwang, J-W. Jaw and A.L. Ch'ng, 8/31/89.

NCEER-89-0029 "Bedrock Accelerations in Memphis Area Due to Large New Madrid Earthquakes," by H.H.M. Hawng, C.H.S. Chen and G. Yu, 11/7/89.

NCEER-89-0030 "Seismic Behavior and Response Sensitivity of Secondary Structural Systems," by Y.Q. Chen and T.T. Soong, 10/23/89.

NCEER-89-0031 "Random Vibration and Reliability Analysis of Primary-Secondary Structural Systems," by Y. Ibrahim, M. Grigoriu and T.T. Soong, 11/10/89.

NCEER-89-0032 "Proceedings from the Second U.S. - Japan Workshop on Liquefaction, Large Ground Deformation and Their Effects on Lifelines, September 26-29, 1989," Edited by T.D. O'Rourke and M. Hamada, 12/1/89.

NCEER-89-0033 "Deterministic Model for Seismic Damage Evaluation of Reinforced Concrete Structures," by J.M. Bracci, A.M. Reinhorn, J.B. Mander and S.K. Kunnath, 9/27/89, to be published.

NCEER-89-0034 "On the Relation Between Local and Global Damage Indices," by E. DiPasquale and A.S. Cakmak, 8/15/89.